

Tetraaminoperylenes: Their Efficient Synthesis and Physical Properties

Lutz H. Gade,^{*,[a]} Christian H. Galka,^[a] Konrad W. Hellmann,^[a] René M. Williams,^[b] Luisa De Cola,^[b] Ian J. Scowen,^[c] and Mary McPartlin^[c]

Abstract: Trimethylsilylation of 1,8-diaminonaphthalene gave 1,8-bis(trimethylsilylamino)naphthalene (**1a**), which was in turn lithiated with two molar equivalents of *n*-butyllithium to give the tris(thf)-solvated dilithium diamide [1,8- $\{(Me_3SiN)Li(thf)_2\}_2C_{10}H_6\}(thf)$ (**2a**). Metal exchange of **2a** with TlCl was carried out in two steps, via the previously characterized mixed-metal amide [1- $\{(Me_3SiN)Li(thf)_2\}_2-8-\{(Me_3SiN)Tl\}-C_{10}H_6\}$, to give the dithallium diamide [1,8- $\{(Me_3SiN)Tl\}_2C_{10}H_6$] (**3a**). Thermolysis of **3a** cleanly gave a 1:1 mixture of the 4,9-bis(trimethylsilylamino)perylenequinone-3,10-bis(trimethylsilylimine) (**4a**) and **1a**. By this route, a whole series of silylated homologues of **4a** was obtained in good yields, while the same method proved to be inefficient for the synthesis of the alkyl-substituted analogues. Compound **4a** and its *tert*-butyldimethylsilyl derivative **4d** were reduced with sodium amalgam to give, after protonation, the corresponding 3,4,9,10-tetraaminoperylenes **7a** and **7d**. Cyclic voltammetry showed two reversible, closely spaced reduction waves ($E_{red1} = -1.39$, $E_{red2} = -1.59$ V versus SCE) corresponding to this conversion. The perylenes **7a** and **7d** are thought to be the primary products in the reaction cascade leading to the perylene derivatives, involving the ther-

mal demetalation of the thallium amides, possibly via $Tl^{II}-Tl^{III}$ intermediates, first to give **7a** and its analogues. The final oxidation of the tetraaminoperylenes by one molar equivalent of **3a** and analogous thallium amides gave the quinoidal derivatives such as **4a** and **4d**, a step that could be studied by direct reaction of the isolated species. The UV/Vis absorption spectra of the 4,9-bis(silylamino)perylenequinone-3,10-bis(silylimines) are characterized by a long-wavelength absorption band with a pronounced vibrational structure ($\lambda_{max} = 639$ nm, $lg \epsilon = 4.53$) attributed to a $\pi^* \leftarrow \pi$ and a $\pi^* \leftarrow n$ absorption band at 454 nm ($lg \epsilon = 4.83$), along with intense absorption in the UV region. A weak red emission with a rather low quantum yield ($\Phi_{fl} = 0.001$, $\lambda_{max} = 660$ nm) is observed upon irradiation of a sample; the lifetime of the emission is only 66 ps. The low emission quantum yield is attributed to the $^* \pi \leftarrow n$ transition of the amino perylene, which induces strong spin-orbit coupling, leading to a large triplet yield. The triplet state was probed by transient absorption spectroscopy and found to have a lifetime of

200 ns in air, and 1100 ns in argon-flushed solution. Treatment of **4a** with a stoichiometric amount of KF in methanol/water under phase-transfer conditions (with the cryptand [C 222]) gave an almost quantitative yield of the parent compound 4,9-diaminoperylenequinone-3,10-diimine (**8**). Treatment of **8** with two molar equivalents of the ruthenium complex $[Ru(bpy)_2(acetone)_2](PF_6)_2$, generated in situ, yielded the blue dinuclear ruthenium complex $[(bpy)_4Ru_2\{\mu_2-N,N':N'',N'''\}-[4,9-(NH_2)_2-3,10-(NH)_2]C_{20}H_8\}](PF_6)_4$ (**9**), the redox properties of which were studied by cyclic voltammetry. The difference in the potentials of the two one-electron redox steps (225 mV) indicates strong coupling of the metal centers through the 4,9-diaminoperylenequinone-3,10-diimine bridging ligand and corresponds to a comproportionation constant K_c of 6.3×10^3 . The UV/Vis absorption spectrum of the mixed valent form, which is stable in air, has a characteristic intervalence charge-transfer (IVCT) band in the near infrared at 930 nm ($lg \epsilon = 3.95$), from which an electronic coupling parameter J of 760 cm^{-1} could be estimated, placing compound **9** at the borderline between the class II and class III cases in the Robin–Day classification.

Keywords: electronic coupling · emission · perylenes · ruthenium · thallium

[a] Prof. L. H. Gade, Dr. C. H. Galka, Dr. K. W. Hellmann
Laboratoire de Chimie Organométallique et de Catalyse (UMR 7513)
Institut Le Bel, Université Louis Pasteur
4, rue Blaise Pascal, 67070 Strasbourg (France)
Fax: (33)390-241531
E-mail: gade@chimie.u-strasbg.fr

[b] Dr. R. M. Williams, Prof. L. De Cola
Molecular Photonic Materials
Institute of Molecular Chemistry, Universiteit van Amsterdam
Nwe Achtergracht 166, 1018 WV Amsterdam (The Netherlands)

[c] Dr. I. J. Scowen, Prof. M. McPartlin
School of Applied Chemistry, University of North London
Holloway Road, London N7 8DB (UK)

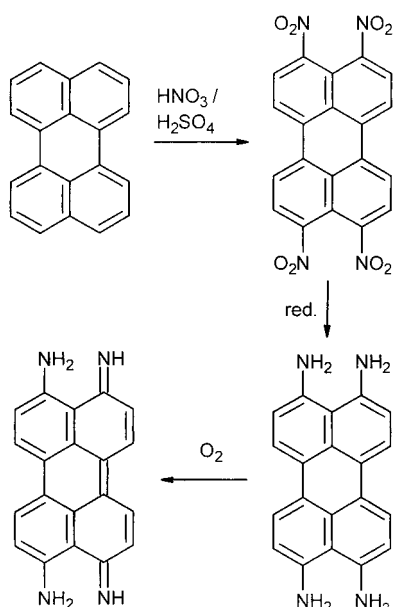
Introduction

Perylenes are “multitalented” chromophores which have attracted interest and found applications well beyond their original role as (mostly) red pigments.^[1,2] These range from uses as laser dyes,^[3] photochemical sensitizers,^[4] absorbers for sunlight collectors^[5] to applications in liquid-crystalline phases^[6] and organic semiconductors.^[7] Moreover, several natural products containing perylene core structures, such as the hypericines^[8] and hypocrellines^[9] have been the objects of systematic studies for use as antiviral or cytostatic agents,^[10]

the latter in particular in the context of use in photodynamic therapy of malignant tumor tissues.^[11]

By far the majority of studies in the field are concerned with the readily accessible perylene tetracarboximides, which are highly photostable fluorescent dyes. Notable contributions to this field originated in Langhals' and Müllen's research groups.^[12] More recently, the corresponding derivatives of the higher "rylenes", the terrylenes and quaterrylenes, have begun to be investigated.^[13]

There are very few examples of tetra-N-substituted perylenes to be found in the literature to date. First attempts date back to 1919, when Zinke and Unterkreuter reported the preparation of 3,4,9,10-tetraaminoperylene, by treatment of the parent compound perylene with concentrated nitric acid (Scheme 1).^[14] A decade later, in 1929, the same group



Scheme 1.

described the reduction of this compound in alkaline solution with Na_2S , NaHSO_3 , or SnCl_2 to give 4,9-diaminoperylenequinone-3,10,-diimine.^[15] This reaction probably proceeded through the 3,4,9,10-tetraaminoperylene, which was then oxidized by air to give the quinoidal product.

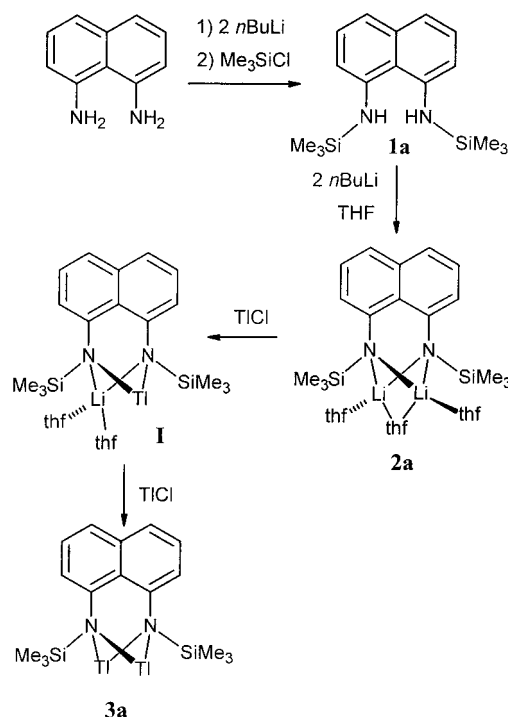
This apparently simple route is in practice cumbersome and gives the desired products in extremely low yields. This may be the reason why the chemistry of aminoperlylenes remains poorly developed in spite of the fact that 4,9-diaminoperylenequinone-3,10,-diimine is the N-analogue of the well-established perylene-related core in oxo-analogues. The latter form the core of the natural products such as the hypericines and hypocrellines mentioned above.

In the course of our investigation into the redox properties of thallium(I) amides we discovered a novel, potentially useful route to the class of 4,9-diaminoperylenequinone-3,10,-diimines.^[16] As will be shown, it is possible to convert these quinoidal systems to the reduced 3,4,9,10-tetraaminoperlylenes, a class of compounds that has very recently been cited

in the patent literature of photovoltaic devices.^[17] Herein we now report a convenient synthesis of novel N-functionalized perylenes, a mechanistic study of their formation and the first results concerning their physical and chemical properties.

Results and Discussion

Synthesis of the 1,8-bis(silylamino)naphthalenes and their lithium amide derivatives, and their conversion into silylated 4,9-diaminoperylenequinone-3,10-diimines: The conversion of 1,8-diaminonaphthalene to 4,9-diaminoperylenequinone-3,10-diimine was achieved in several steps. Trimethylsilylation of the primary diamine gave the 1,8-bis(trimethylsilylamino)-naphthalene **1a** (Scheme 2), which in turn was lithiated with



Scheme 2. Synthesis of the dithallium diamide **3a**.

two molar equivalents of *n*-butyllithium to give the tris(thf)-solvated lithium amide $[1,8\text{-}((\text{Me}_3\text{SiN})\text{Li}(\text{thf})_2)\text{C}_{10}\text{H}_6](\text{thf})$ (**2a**). Metal exchange of **2a** with TlCl was carried out in two steps, via the previously characterized mixed metal amide $[1\text{-}((\text{Me}_3\text{SiN})\text{Li}(\text{thf})_2)\text{-}8\text{-}((\text{Me}_3\text{SiN})\text{Tl})\text{C}_{10}\text{H}_6]$ (**I**),^[18] to give the dithallium diamide $[1,8\text{-}((\text{Me}_3\text{SiN})\text{Tl})_2\text{C}_{10}\text{H}_6]$ (**3a**).

The orange thallium amide **3a** was found to be only sparingly soluble in aromatic solvents, in which it is relatively stable. We attribute this low solubility to a polymeric structure of the crystalline compound due to Tl-arene stacking of the type found by X-ray diffraction for the dimeric mixed amide **I**.^[18, 19] Heating of compound **3a** in 1,4-dioxane for 17 h resulted in its complete conversion into a 1:1 mixture of diamine **1a** and the new 4,9-bis(trimethylsilylamino)perylenequinone-3,10-bis(trimethylsilylimine) **4a**. Monitoring of this last reaction step by ¹H NMR spectroscopy clearly

demonstrated the high selectivity of this conversion, as apparent from a series of spectra recorded during the course of thallium amide thermolysis carried out in an NMR spectrometer (Figure 1).

In the NMR spectra, the signals of the starting material and both products are visible, while by-products or long-lived intermediates are clearly absent. To assess the generality of this conversion a series of 1,8-bis(silylamino)naphthalenes **1a–1f** was synthesized and metalated to give the corresponding thf-solvated lithium amides **2a–2f**. By heating with TlCl in 1,4-dioxane for 16–44 h, these were then directly converted into 1:1 mixtures of the diaminonaphthalenes and the 4,9-bis(silylamino)perylenequinone-3,10-bis(silylimines) **4a–4f** (Scheme 3). We were able to develop reaction conditions under which the transformation of the 1,8-diaminonaphthalene could be converted in a one-pot procedure (by sequential metalation, metal exchange and thermolysis) to give overall yields of the silyl-substituted perylenes of 75–82% (with reference to the maximum amount of diaminonaphthalene convertible into the perylene: i.e., two out of three molecules).

The differences in the reaction times were mainly due to the ease with which the Li/Tl exchange took place, which was in turn dependent upon the size of the silyl groups attached to the amido-N atoms. The different degrees of exposure of the N-coordinated metal ions are already reflected in the degree of solvation by the donor solvent THF. Whereas the dilithium diamide obtained by metalation of **1a** in THF was isolated and characterized as a solvate with a variable number of thf co-ligands depending on the reaction conditions,^[18, 20] the metalation of **1c** exclusively gave the bis(solvate) **2c**. Its crystal structure was determined by X-ray diffraction, and its molecular structure is depicted in Figure 2.

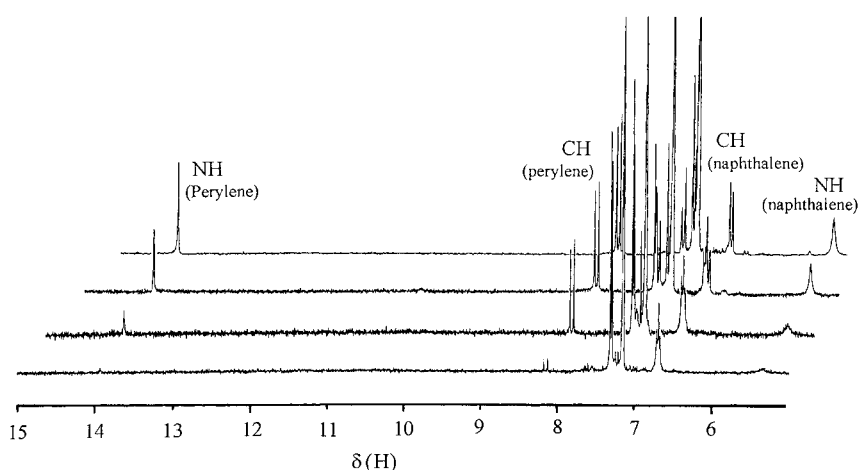
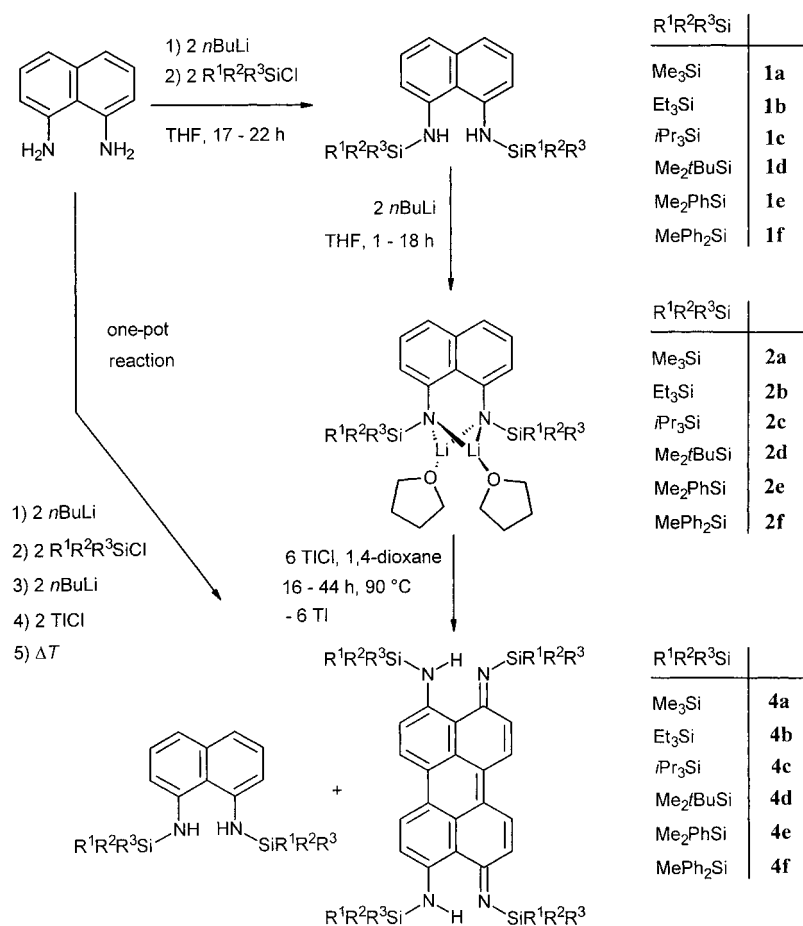


Figure 1. Series of ^1H NMR spectra recorded during the thermal decomposition of **3a** in C_6D_6 at 63°C . The four spectra were recorded after (from bottom to top): 5 min, 60 min, 285 min, 28 h.



Scheme 3. General preparative scheme for the synthesis of the 4,9-bis(silylamino)perylenequinone-3,10-bis(silylimines) **4a–4f**.

As found for most chelate dilithium diamides,^[20, 21] the structural centerpiece is the cyclic Li_2N_2 unit. The detailed structural arrangement is determined both by the rigid aromatic ligand backbone (the central C(5)–C(6) bond of which lies on a crystallographic C_2 axis) and the two $i\text{Pr}_3\text{Si}$ groups at the amido-N atoms. The bulky silyl groups shield the

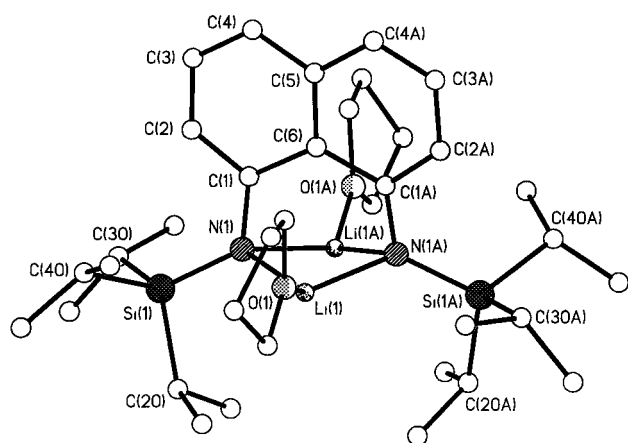
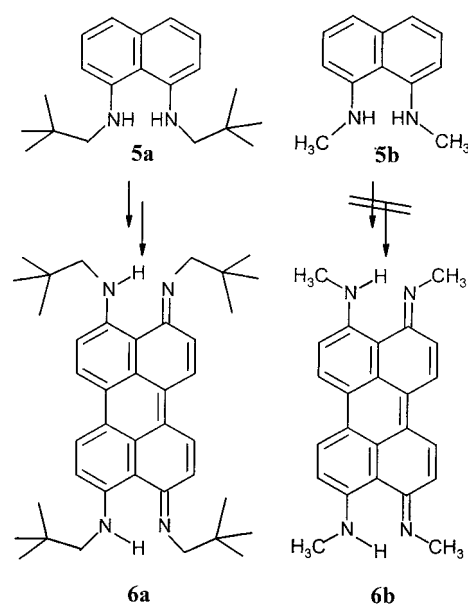


Figure 2. Molecular structure of the lithium amide **2c**. Selected bond lengths [Å] and angles [°]: Li(1)–N(1) 2.024(5), Li(1)–O(1) 1.906(5), Si(1)–N(1) 1.724(2) Si(2)–N(2) 1.737(3), N(1)–C(1) 1.405(4), N(2)–C(7) 1.405(4), C(1)–C(2) 1.397(4), C(1)–C(6) 1.478(3), C(2)–C(3) 1.389(4), C(3)–C(4) 1.368(4), C(4)–C(5) 1.419(4); Si(1)–N(1)–C(1) 122.9(2), C(1)–C(6)–C(7) 126.3(3), C(4)–C(5)–C(10) 116.9(4), C(2)–C(1)–C(6) 117.4(3), C(1)–C(2)–C(3) 123.7(3), C(2)–C(3)–C(4) 120.4(3), C(3)–C(4)–C(5) 119.8(3), C(4)–C(5)–C(6) 121.6(2), C(5)–C(6)–C(1) 116.8(2), Li(1)–N(1)–Li(1A) 85.1(2), N(1)–Li(1)–N(1A) 91.5(2).

two lithium centers, which explains the reduced reactivity of this compound in the metal exchange with TiCl₄ in comparison with **2a**. Both Li–N distances ($d(\text{Li}(1)\text{--N}(1))$ 2.023(5), $d(\text{Li}(1)\text{--N}(1A))$ 2.028(5) Å) lie in the usual range to be expected for such compounds.^[22] In each molecule both silyl groups are slightly, and unequally, twisted out of the naphthalene plane, with the two Si atoms lying on opposite sides (deviations from the arene plane Si(1) = –0.08 and Si(2) = +0.42 Å), while the two thf coligands lie on the opposite side of the Li₂N₂ ring towards the arene ring system, thus minimizing contact with the bulky silyl substituents.

The transformation of the diamidonaphthalenes appeared to depend upon the presence of the N-bound silyl substituents. Attempts to convert 1,8-diamidonaphthalene directly to the corresponding parent perylene did not give the desired coupling product. The replacement of the silyl substituents by alkyl substituents led to a significant decrease in the yields of coupled naphthalenes, as was established—among other examples—for the sequential lithiation, metal exchange and thermolysis of 1,8-bis(neopentylamino)naphthalene (**5a**).^[23] The bis-thf solvated lithium amide of this amine was heated in the presence of a stoichiometric amount of TiCl₄ to give a reaction mixture of the perylene **6a** (in up to 21% yield), the diamidonaphthalene starting material **5a** and other unidentified products. In contrast, no perylene derivative could be identified upon similar treatment of 1,8-bis(methylamino)-naphthalene **5b** (Scheme 4).

Crystal structures of the silylated 4,9-diaminoperylenequinone-3,10-diimines 4a and 4d: The patterns of bond lengths in the molecular structures of **4a** and **4d** are similar, but because of poor diffraction by the crystals of **4a**, possibly caused by considerable rotational disorder of the trimethylsilyl groups, the esds in compound **4a** are relatively high and preclude detailed discussion.



Scheme 4. Conversion and attempted conversion of **5** and **5a**, respectively, into the corresponding perylenequinones.

The molecular structure of one of the two independent molecules in the asymmetric unit of crystalline **4d** is illustrated in Figure 3. The chemically equivalent bond lengths in the two independent molecules, and the corresponding bond lengths on the two sides within each molecule,

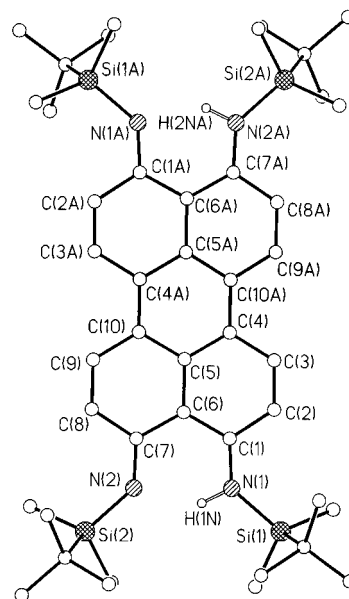


Figure 3. Molecular structure of **4d**. Selected bond lengths [Å] and angles [°]: Si(1)–N(1) 1.744(3), Si(2)–N(2) 1.744(3), N(1)–C(1) 1.334(4), N(2)–C(7) 1.329(4), C(1)–C(2) 1.433(5), C(1)–C(6) 1.436(5), C(2)–C(3) 1.340(5), C(3)–C(4) 1.421(5), C(4)–C(5) 1.419(5), C(4)–C(10') 1.421(5), C(6)–C(7) 1.438(4), C(7)–C(8) 1.431(4), C(8)–C(9) 1.343(4), C(9)–C(10) 1.425(4), C(10)–C(5) 1.420(4); Si(1)–N(1)–C(1) 133.9(2), Si(2)–N(2)–C(7) 133.7(2), C(1)–C(6)–C(1A) 121.2(3), C(4)–C(5)–C(4A) 118.1(3), C(2)–C(1)–C(6) 117.1(3), C(8)–C(7)–C(6) 116.9(3), C(1)–C(2)–C(3) 122.8(3), C(7)–C(8)–C(9) 122.7(3), C(2)–C(3)–C(4) 122.3(3), C(8)–C(9)–C(10) 122.5(3), C(3)–C(4)–C(5) 117.5(3), C(9)–C(10)–C(5) 117.2(3), C(4)–C(5)–C(6) 121.0(3), C(10)–C(5)–C(6) 120.9(3), C(5)–C(6)–C(1) 119.2(3), C(5)–C(6)–C(7) 119.7(3), C(5)–C(4)–C(10A) 121.1(3)

are equal within experimental error. The molecules have a virtually planar ring systems (mean maximum deviation from planarity 0.06 Å). The direct location of the hydrogen atoms on both amino nitrogen atoms of the independent half molecule indicates that the solid-state structure is the result of a 50:50 disorder of the two tautomers. There are significant differences in the bond lengths relative to the reported values for the parent compound perylene. In particular, the mean lengths of C(2)–C(3) and C(8)–C(9) (1.341 Å) and C(4)–C(10') (1.421 Å) are considerably shorter than the analogous values in perylene (1.40 and 1.48 Å, respectively). A similar shortening of these bonds has been observed previously for the perylene dianion, in which the respective mean values are 1.37 and 1.43 Å,^[24] as well as in the hydroxyperylenequinones constituting the cores of the hypocrellines.

The crystal structures of polyaromatics have attracted considerable attention in recent years, in order to demonstrate the utility and power of theoretical structure prediction tools. This development was supplemented by the proposal of classification schemes for the arrangement of such polyaromatics in crystals.^[25] The solid-state structures of a large number of biscarboximide perylene derivatives have been studied in order to investigate the correlation between molecular packing and color in pigments.^[26] In most cases, stacked “face-to-face” arrangements (separations of between 3.345 and 3.476 Å between the parallel oriented ring systems) of perylenes are found, provided that there are no bulky substituents preventing this. A rare, if not unique, example for the latter situation is the bis(2,6-dimethylphenylcarboximido)perylene reported by Graser and Hädicke.^[27]

The crystal structures in this study are markedly different from those of the carboximido derivatives and were found to display no “face-to-face” interactions. Instead, there are close alkyl to aromatic ring contacts in the butyldimethylsilylated derivative **4d** (Figure 4a), with neighbouring molecules being oriented almost perpendicularly to each other (dihedral angle between the ring systems of two neighbouring molecules: 92.7°). This arrangement is analogous to the γ -type in Desiraju's system of classification.^[28] In contrast to this, the aromatic ring systems of adjacent molecules in **4a** exhibit “edge-to-face” interaction (Figure 4b), resulting in an overall “herring-bone” arrangement in the crystal.

Reduction of the 4,9-diaminoperylenequinone-3,10-diimines 4a and 4d to give the corresponding 3,4,9,10-tetraaminoperlylenes 7a and 7d: Treatment of **4a** and **4d** with two molar equivalents of sodium amalgam and subsequent addition of two equivalents of NEt_3HCl in THF gave the extremely air-sensitive, strongly fluorescing tetraaminoperlylenes **7a** and **7d** as brick-red microcrystalline solids (Scheme 5).

The relatively modest yields of 40–50% are due to practical difficulties associated with the extreme air-sensitivity of these perylenes. The most characteristic changes in the ^1H NMR spectra of the reduced perylene forms with respect to those of the quinoidal systems are the significant shifts of all proton resonances to low field, the reduction of the $^3J(\text{H,H})$ coupling constant of the aromatic protons by 1.6 Hz and the observation of the NH-proton signals at $\delta = 5.43/5.29$ (**7a/7d** in C_6D_6) instead of at $\delta = 14.13/13.42$ (**4a/4d**).

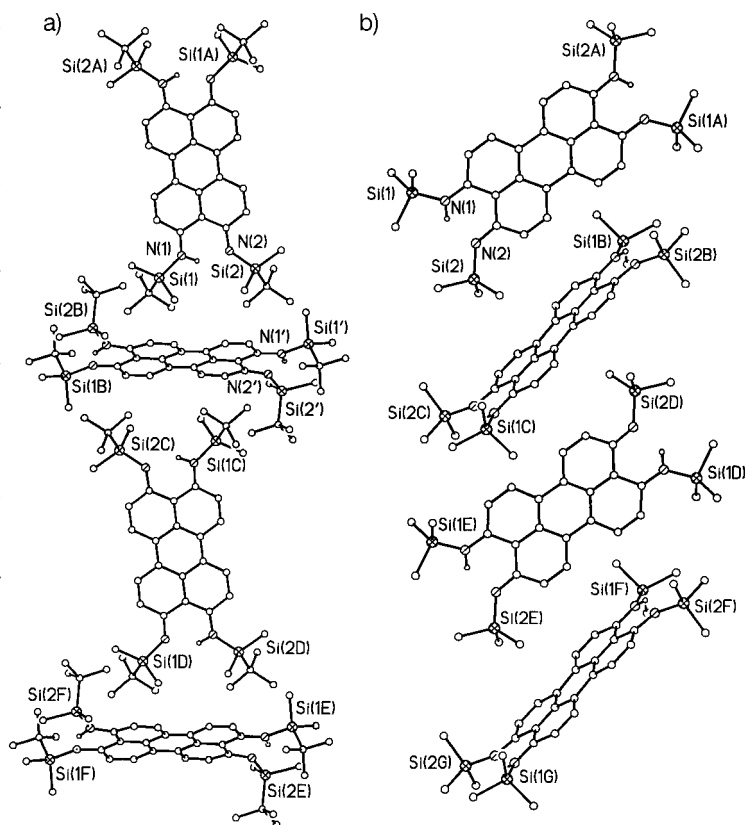
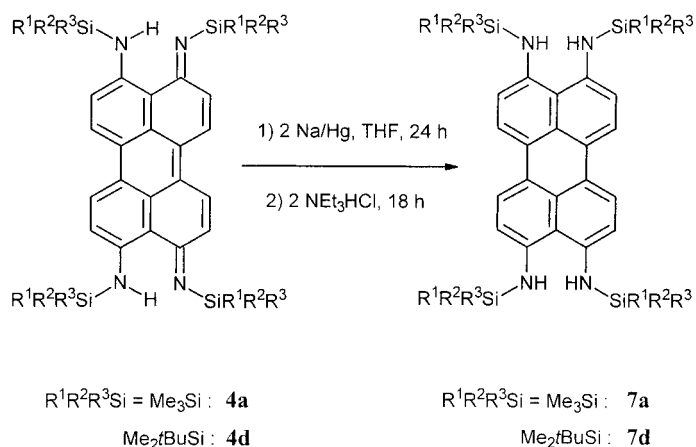
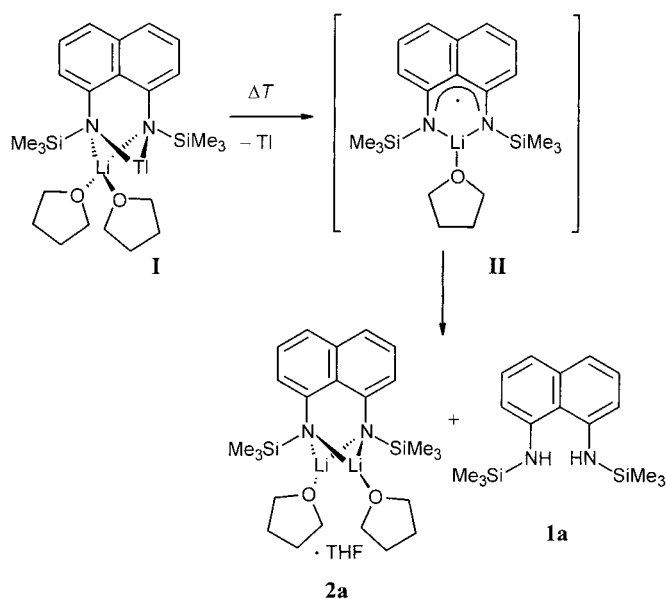


Figure 4. The packing patterns of **4a** (a) and **4d** (b) in the crystal.



Scheme 5. Reduction of **4a** and **4d** to give the tetraaminoperlylenes **7a** and **7d**.

Aspects of the mechanism of the thallium-induced coupling of 1,8-diaminonaphthalenes: The details of the thermal conversion of the thallium amide derivatives of the 1,8-bis(silylamino)naphthalenes to give the quinoidal perylenes **4a–4f**, discussed above, provide some indications concerning the mechanism of the coupling reaction. First, the coupled perylene derivatives are exclusively obtained from the dithallium diamides; secondly, thermolysis of the mixed diamide [1-((Me_3SiN) $\text{Li}(\text{thf})_2$)-8-((Me_3SiN) Tl) C_{10}H_6] (**I**) gave a 1:1 mixture of **1a** and **2a**, most probably via a short-lived radical intermediate **II** (Scheme 6).

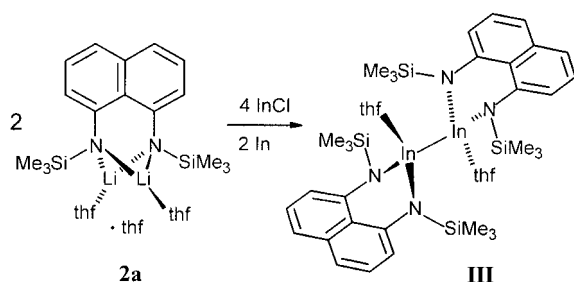


Scheme 6. Thermal degradation pathway of the previously reported mixed lithium/thallium amide **I**.

All attempts to detect radical intermediates in this and other reactions of the naphthalene derivatives, either directly by ESR spectroscopy or by observation of a CIDNP effect at variable temperatures and magnetic field, failed, most probably due to their short-lived nature.

The coupling of the two diamionaphthalene units is thought to occur subsequent to the thermal demetalation of the thallium amides, with the pure metal immediately precipitating from the reaction mixture. Monitoring of this reaction by NMR spectroscopy, as shown in Figure 1, while varying the initial concentration of the thallium amide **3a** gave a first-order rate law. Since the rate-determining step is most likely to be associated with the initial demetalation, this observation is of limited value for a mechanistic proposal.

In principle, the coupling step may involve two free diradical species, a notion that appears to contradict the high selectivity of the reaction. Alternatively, it may proceed in a two-step reaction process through a metal–metal bonded dithallium(II) intermediate, analogously to the recently characterized diindium complex [1,8-((Me₃SiN)₂In(thf))]-C₁₀H₆₂(*In-In*) (**III**), which is the exclusive product of the reaction of **2a** with InCl (Scheme 7).^[16]

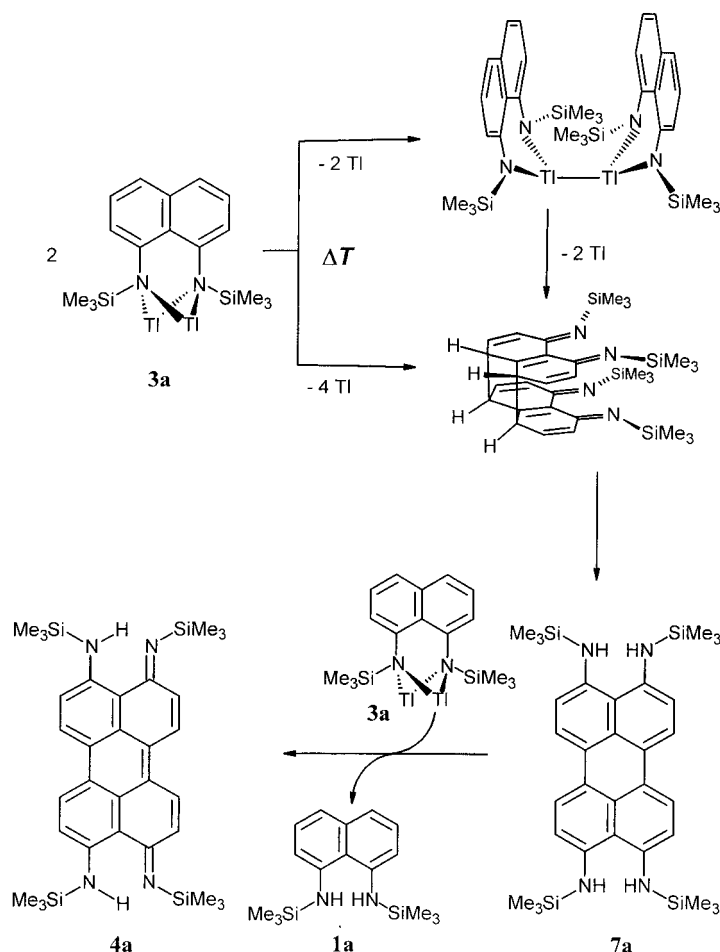


Scheme 7. The previously reported synthesis of the In^{II}–In^{II} complex **III**.

We have previously demonstrated the accessibility of such a divalent Tl^{II}–Tl^{II} compound by the isolation and structural characterization of the first thallium(II) amide containing a covalent Tl–Tl bond.^[29] In such a dinuclear intermediate, which is thought to be very short-lived under the reaction conditions of the perylene synthesis, the two naphthalene molecules are pre-oriented with respect to each other, which in turn facilitates the coupling in the second demetalation step.

The most important observation is the exact stoichiometry in the conversion of three molar equivalents of the thallium amide, such as **3a**, to give the 1:1 mixture of **1a** and **4a**, a product ratio that remains unchanged throughout the course of the reaction. Moreover, the quinoidal perylenes **4a–4f** are not the direct coupling products of two 1,8-diamionaphthalene derivatives, but rather subsequently oxidized forms. It is thus likely that the third molar equivalent of thallium amide is consumed in this oxidation step. This could be shown directly by treatment of the reduced 3,4,9,10-tetrakis(trimethylsilylamino)perylene (**7a**) with an equimolar amount of thallium amide **3a**, which cleanly gave **4a**.

From these observations we propose the reaction mechanism shown in Scheme 8 to account for the observations discussed above.



Scheme 8. Proposed mechanistic scheme for the conversion of the thallium amide **3a** into the corresponding perylenequinone **4a** via the reduced perylene **7a**.

We note that our mechanistic proposal bears a formal similarity to the well established benzidine rearrangement, although the latter is a cation-induced (proton-induced) reaction, in contrast to the case at hand. This analogy is consistent with the observation that the bulky silyl groups appear to be necessary in the coupling reaction leading to **4a–4f**, preventing potential couplings in the 2- and 7-positions.

Photo- and electrochemical properties of compound **4d**:

Since the quinoidal perylenes **4a–4f** reported in this work display very similar absorption spectra, we decided to investigate the 4,9-diaminoperylenequinone-3,10-diimine **4d** more closely. As is the case for the other derivatives, this compound is a black-green, highly crystalline solid with a purple lustre. In solution it displays a beautiful deep-green color. The UV/Vis absorption spectrum recorded in benzene is shown in Figure 5, with maxima at 299, 454, 548, 590 and

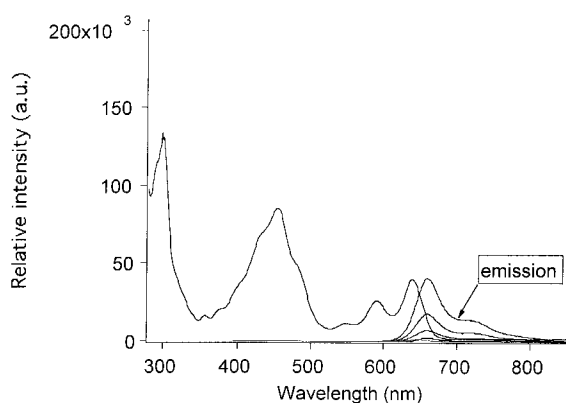


Figure 5. UV/Vis absorption and emission spectra of compound **4d** in benzene. The incremental time delay of the emission spectra is 1 ns (gate 5 ns).

639 nm ($\lg \epsilon = 5.10, 4.83, 3.89, 4.31$ and 4.53). The latter three absorption maxima represent a vibrational progression ($\tilde{\nu} = 1270 \text{ cm}^{-1}$) of an absorption band which we believe to be due to a $\pi^* \leftarrow \pi$ transition of the type observed at lower wavelengths in most perylene derivatives. Whereas the position of this band remains essentially unaltered upon going from pentane ($\epsilon_r = 1.0$) to dichloromethane ($\epsilon_r = 8.9$) to dimethyl sulfoxide ($\epsilon_r = 47.0$), the more intense band at 454 nm, for which there is no correspondence in the well studied perylene carboximide derivatives, experiences a small but measurable shift ($\Delta\tilde{\nu} = 460 \text{ cm}^{-1}$). We assign this to a transition with a certain degree of $\pi^* \leftarrow n$ character involving the lone pairs on the N-functional groups.

A weak red emission with a very low quantum yield ($\Phi_{\text{fl}} = 0.001$, $\lambda_{\text{max}} = 660 \text{ nm}$) is observed upon irradiation of a sample. The fact that the perylene itself is the emitter was substantiated by the excitation-emission spectra, which also indicated that the emission, which displays a vibrational progression of $\tilde{\nu} \approx 1200 \text{ cm}^{-1}$, arises after excitation of both the $\pi^* \leftarrow \pi$ and the $\pi^* \leftarrow n$ transitions. From the 639 nm absorption maximum and the maximum of the emission (660 nm) we obtain a considerable Stokes shift of 497 cm^{-1} , indicating a nuclear

configuration in the first excited singlet state substantially different from that in the ground state. From the overlap of the two spectra the singlet state energy is determined to be 649 nm (${}^1E_{00} = 1.91 \text{ eV}$). The lifetime of the emission is only 66 ps, as inferred from time-correlated single-photon counting experiments (Figure 6). It is thus evident that the photo-

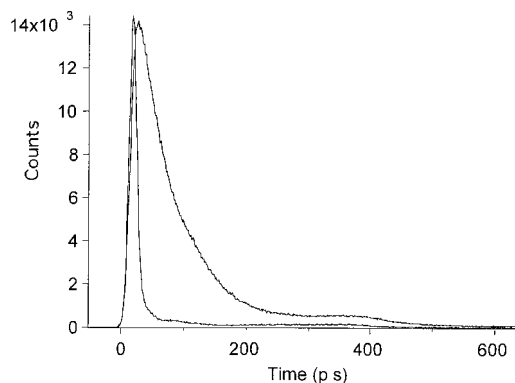


Figure 6. Time-resolved emission of compound **4d** in benzene observed with time-correlated single-photon counting ($\tau = 66 \pm 5 \text{ ps}$). Excitation 324 nm, observation at 680 nm. The Instrument Response Function (FWHM 20 ps) obtained by observation of the Raman band of water at 363.5 nm is also shown.

physics of the amino perylene are very different from those of perylenebisimides, or perylene itself. Perylenebisimides are characterized by very high quantum yields of emission ($\Phi_{\text{fl}} \approx 1$) with lifetimes of about 3.5 ns, which appear to be fairly substituent- and solvent-independent.^[30] This property, together with their lightfastness, makes them appropriate as laser dyes or fluorescent labels, and only aggregation or the incorporation of electron donors can change this high emission yield.^[31] The photophysics of perylene itself are slightly solvent-dependent, and also characterized by a high emission quantum yield ($\Phi_{\text{fl}} = 0.75$ to 0.87 , $\tau = 6 \text{ ns}$) and a low triplet yield ($\Phi_{\text{T}} = 0.014$ to 0.0088).^[32]

Clearly the $\pi^* \leftarrow n$ transition of the amino perylene studied here induces strong spin-orbit coupling, leading to a large triplet yield and the almost complete absence of emission. The triplet state plays a major role in the relaxation processes after excitation and a very intense transient absorption spectrum is observed, with a lifetime of 200 ns in air and 1100 ns in argon-flushed solution. Furthermore, strong ground-state bleaching is apparent, with identical lifetimes of the bleaching and absorption bands and isoabsorptive points, at which ground and excited states have equal extinction coefficients (Figure 7).

Cyclic voltammetry (in tetrahydrofuran) shows two reversible, closely spaced reductions ($E_{\text{red}1} = -1.39$, $E_{\text{red}2} = -1.59 \text{ V}$ versus SCE) and an irreversible oxidation. It appears that the quinoidal structural elements in **4d** are not reflected in any particular ease of reduction. Upon electrochemical reduction a small hypsochromic shift (639–606 nm) is already observable at low potentials (-0.3 V , no current), indicating a field or deposition effect at the electrodes (Figure 8).

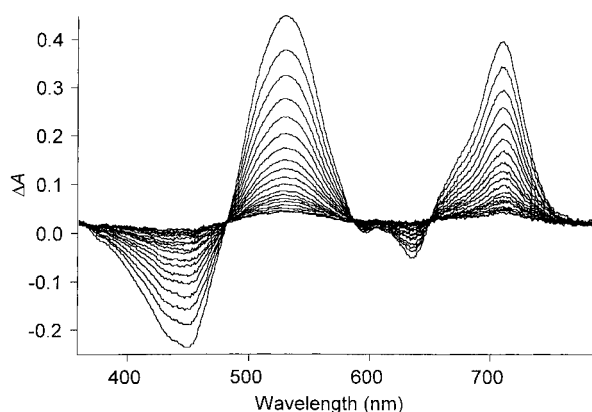


Figure 7. Transient absorption spectra of compound **4d** in benzene obtained with the OMA set-up. Excitation at 450 nm. The incremental time delay is 40 ns.

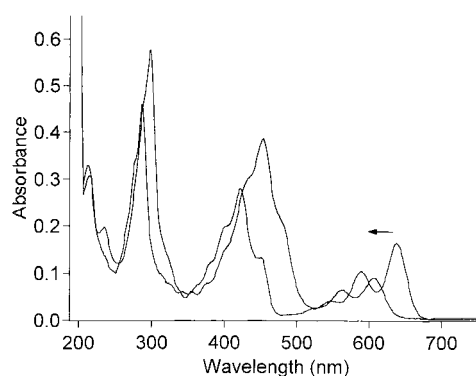


Figure 8. Shift of the UV/Vis absorption spectrum of compound **4d** in tetrahydrofuran, observed in the spectroelectrochemical cell, at the start of reduction to about -0.3 V versus SCE.

Upon further reduction, strong spectral shifts are recorded, with isosbestic points at 263 and 461 nm, and the generation of a new, broad and strong absorption in the red, centered around 624 nm, accompanied by a decrease in the 290 and 450 nm bands. The final spectrum corresponds to the doubly reduced species (Figure 9).

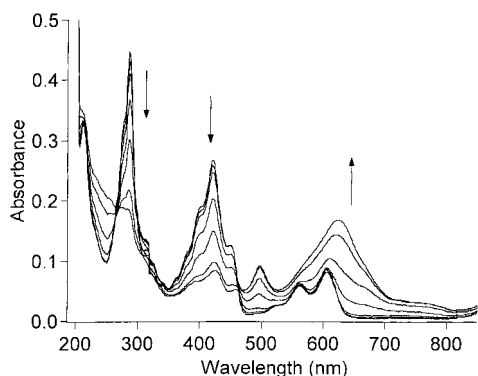
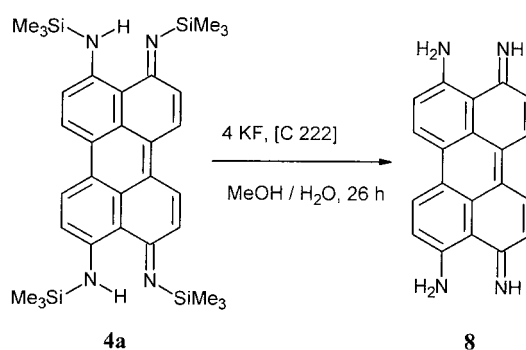


Figure 9. Changes in the UV/Vis absorption spectrum of compound **4d** in tetrahydrofuran, observed in the spectroelectrochemical cell, upon total double reduction of the compound.

Synthesis and characterization of the parent 4,9-diaminoperylenequinone-3,10-diimine and its properties as a bridging ligand in a Ru_2 complex: In the large majority of metal complexes containing perylenes as ligands, these bind to the metal centers as π -arenes.^[33] It was only very recently that Würthner and co-workers reported the first examples of perylenebisimides as bridging ligands in Pd and Pt complexes in which the metals are σ -bonded to the functional groups of the perylene derivatives.^[34] The presence and relative arrangement of the four nitrogen functional groups in the silylated 4,9-diaminoperylenequinone-3,10-diimine derivatives makes them potential bridging ligands. This in turn may provide additional information on their electronic structure, through study of the degree of electronic communication between two metal centers linked by such a perylene.

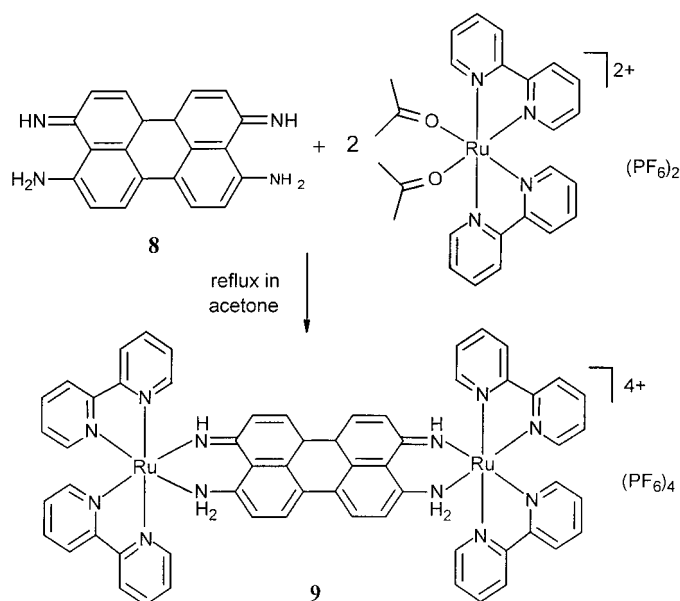
Since the silyl groups effectively shield the N-donor atoms it was necessary to remove these Si-substituents by treatment with a stoichiometric amount of KF in methanol/water under phase-transfer conditions (with the cryptand [C 222]). Applied to bis(trimethylsilylamino)-perylenequinone-3,10-bis(trimethylsilylimine) (**4a**), this method gave an almost quantitative yield of the parent compound 4,9-diaminoperylenequinone-3,10-diimine (**8**) (Scheme 9).



Scheme 9. Desilylation of **4a** to give the parent [4,9-(NH_2)₂-3,10-(NH)₂]C₂₀H₈ (**8**).

Treatment of compound **8** with two molar equivalents of the ruthenium complex $[Ru(bpy)_2(acetone)_2](PF_6)_2$,^[35] generated in situ, and heating under reflux for 90 h cleanly gave the blue dinuclear ruthenium complex $[(bpy)_4Ru_2\{\mu_2-N,N':N'',N'''\}-[4,9-(NH_2)_2-3,10-(NH)_2]C_{20}H_8\}](PF_6)_4$ (**9**) (Scheme 10). Because of the presence of two chiral Ru centers, a mixture of the $\Delta\Delta$, $\Lambda\Lambda$ and $\Delta\Lambda$ stereoisomers was obtained. We did not attempt to separate this mixture.

The proposed structure of **9** was supported by the elemental analysis and the electrospray mass spectrum, in which the molecular ion of the diruthenium tetracation was observed at m/z 284.3, as expected. The perylene proton signals of the two diastereomers are not resolved in the 1H NMR spectrum of **9** (δ = 6.86, 9.13; $^3J_{H,H}$ = 10 Hz), and it is only their increased half-widths relative to those of the free ligand that indicate the presence of two isomeric forms. The appropriate sets of proton and ^{13}C NMR resonances for the bpy ligands and the bridging perylene were observed in the 1H and ^{13}C NMR spectra, the observation of a broad vibrational band at



Scheme 10. Synthesis of the dinuclear ruthenium complex $[(\text{bipy})_4\text{Ru}_2\{\mu_2\text{-}N,N':N'',N'''\text{-}[4,9\text{-}(\text{NH}_2)_2\text{-}3,10\text{-}(\text{NH})_2\text{C}_{20}\text{H}_8\}]\text{(PF}_6)_4$ (**9**).

3448 cm^{-1} in the infrared spectrum indicating the presence of the N–H protons at the ligand donor functions of the perylene.

To assess the redox behavior of **9** and the degree of coupling between the two ruthenium centers, a cyclic voltammogram study of the complex was carried out. A cyclic voltammogram recorded at a sweep rate of 100 mVs^{-1} , representing the second cycle, is displayed in Figure 10. The two reversible redox waves with half wave potentials at $+135\text{ mV}$ and at -90 mV correspond to the one-electron reduction steps:

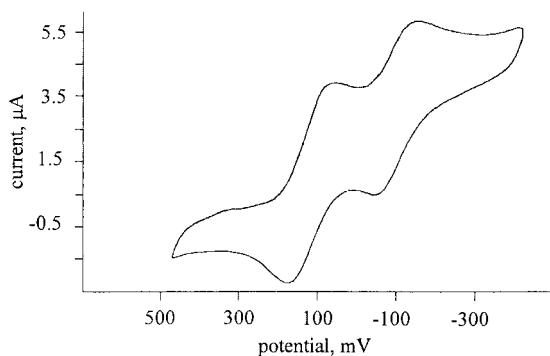
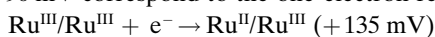


Figure 10. Cyclic voltammogram of the dinuclear ruthenium complex **9** recorded in acetonitrile (scan rate 100 mVs^{-1} , reference electrode Ag/AgCl).

The difference in the potentials of the two one-electron redox steps, of 225 mV , indicates strong coupling of the metal centers through the 4,9-diaminoperylenequinone-3,10-dimine bridging ligand and corresponds to a comproportionation constant K_c of 6.3×10^3 .^[36]

The reduction, if carried out stoichiometrically, is accompanied by a marked change in color of the solution, from deep red for the $\text{Ru}^{\text{III}}/\text{Ru}^{\text{III}}$ form, via the purple mixed-valent complex to the blue reduced species originally isolated. The UV/Vis absorption spectrum of the mixed valent form, which is stable in air, has a characteristic intervalence charge-transfer (IVCT) band in the near infrared at 930 nm ($\lg \epsilon = 3.95$), the intensity of which is another indication of strong coupling through the perylene ligand (Figure 11). The slight deviation from an ideal Lorentzian shape can be seen as arising from the lower than octahedral symmetry at the metal centers and the presence of two diastereomers in solution.

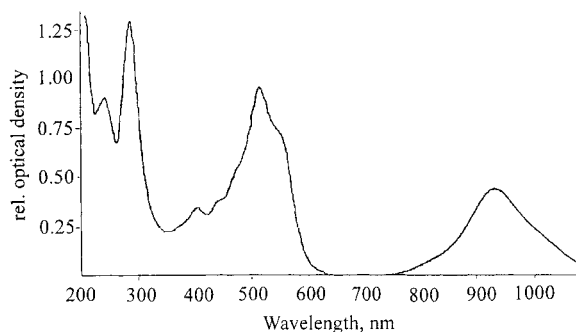


Figure 11. UV/Vis-NIR absorption spectrum of the $\text{Ru}^{\text{II}}/\text{Ru}^{\text{III}}$ mixed-valence derivative of complex **9**, showing the intense IVCT band at 930 nm (recorded in DMSO).

Given the molar extinction coefficient of $8.9 \times 10^3\text{ Lmol}^{-1}\text{cm}^{-1}$, the energy at the maximum of the IVCT band of $10.7 \times 10^3\text{ cm}^{-1}$, the width at half height of 1430 cm^{-1} and an estimated intermetallic distance of 10 \AA , the coupling parameter (J) may be estimated as 760 cm^{-1} .^[36] In the Robin–Day classification,^[37] compound **9** thus represents a system at the borderline between the class II and the class III cases. Because of the limited solubility of the complex, a systematic study of the influence of solvent polarity on the position of the intervalence band was not possible.

Conclusion

In this first systematic study into the preparation and the properties of a new class of amino-functionalized perylenes we have established their principal photo- and redox-chemical properties. These proved to be markedly different to those of the well established and intensely studied tetracarboxybis-imides, which have found a variety of applications in recent years. In addition, we have presented an initial assessment of the ligand properties of 4,9-diaminoperylenequinone-3,10-dimine, the parent compound, which promises a rich and varied coordination chemistry in polynuclear arrays. Its use as a “building block” in ordered molecular arrays is currently being explored.

The thallium-induced coupling of 1,8-diaminonaphthalene derivatives has provided an efficient route to the amino-functionalized perylenes, which can now readily be synthesized in $10\text{--}50\text{ g}$ quantities. In the further development of this

coupling reaction, our main aim will be to replace the poisonous thallium reagents by other redox-active metals while retaining the high selectivity of the conversion. Given the specific structural characteristics of thallium in its different oxidation states, this may require a major effort.

Experimental Section

All manipulations were performed under an inert gas atmosphere of dried argon in standard (Schlenk) glassware, which was flame-dried with a Bunsen burner prior to use. Solvents were dried according to standard procedures and saturated with Ar. The deuterated solvents used for the NMR spectroscopic measurements were degassed by three successive “freeze–pump–thaw” cycles and dried over 4 Å molecular sieves. Solids were separated from suspensions by centrifugation, thus avoiding filtration procedures. The centrifuge employed was a Rotina 48 (Hettich Zentrifugen, Tuttlingen, Germany) equipped with a specially designed Schlenk tube rotor.

^1H , ^{13}C , ^{29}Si , and ^7Li NMR spectra were recorded at 200.13, 50.32, 39.76 and 77.77 MHz, respectively, on a Bruker AC 200 spectrometer equipped with a B-VT-2000 variable-temperature unit and with tetramethylsilane or Li/H₂O (1m) as reference. The IR spectra were recorded on a Bruker IFS 25 FT-IR spectrometer.

Elemental analyses were carried out in the microanalytical laboratory of the chemistry department at Würzburg. All starting materials were obtained commercially and used without further purification.

General procedure for the preparation of the 1,8-bis(silylamino)naphthalenes: A solution of *n*-butyllithium in *n*-hexane (2.5M, 40.0 mL, 100.0 mmol) was added dropwise at -30°C to a solution of 1,8-(H₂N)₂C₁₀H₆ (7.91 g, 50.0 mmol) in THF (80 mL). The reaction mixture was allowed to warm to ambient temperature and, after the evolution of butane had subsided, was briefly heated under reflux. After the mixture had again been cooled to -30°C a solution of the respective chlorosilane (100.0 mmol) in THF (60 mL) was slowly added. After the reaction mixture had been stirred for 19 h at ambient temperature, the solvent was removed in vacuo and the residue was extracted with *n*-pentane (65 mL; for **1a–1d**) or toluene (30 mL; for **1e** and **1f**) as off-white solids.

1,8-(Me₃SiNH)₂C₁₀H₆ (1a): Yield: 15.1 g (100%); m.p. 44°C ; ^1H NMR (200.13 MHz, CDCl₃, 295 K): $\delta = 0.29$ (s, 18H; Si(CH₃)₃), 5.55 (brs, 2H; NH), 6.71 (dd, $^3J_{\text{Ha,Hb}} = 6.8$ Hz, $^4J_{\text{Ha,Hc}} = 1.8$ Hz, 2H; H^a, C₁₀H₆), 7.15–7.27 ppm (m, 4H; H^b + H^c, C₁₀H₆); ^{13}C NMR (50.32 MHz, CDCl₃, 295 K): $\delta = 0.0$ (Si(CH₃)₃), 115.2 (CH; C₁₀H₆), 120.2 (CH; C₁₀H₆), 121.1 (C; C₁₀H₆), 125.6 (CH; C₁₀H₆), 137.3 (C; C₁₀H₆), 144.3 ppm (CN; C₁₀H₆); ^{29}Si NMR (39.76 MHz, CDCl₃, 295 K): $\delta = 3.7$ ppm; IR (KBr): $\tilde{\nu} = 3310$ (w), 3210 (w), 2880 (w), 2840 (w), 1570 (s), 1510 (w), 1410 (m), 1305 (m), 1290 (m), 1245 (s), 1035 (m), 875 (vs), 865 (vs), 840 (vs), 750 cm⁻¹ (m); elemental analysis calcd (%) for C₁₆H₂₆N₂Si₂ (302.57): C 63.52, H 8.66, N 9.26; found: C 63.36, H 8.58, N 9.19.

1,8-(Et₃SiNH)₂C₁₀H₆ (1b): Yield: 3.86 g (100%); m.p. 18°C ; ^1H NMR (200.13 MHz, CDCl₃, 295 K): $\delta = 0.79$ (q, $^3J_{\text{H,H}} = 7.5$ Hz, 12H; Si(CH₂CH₃)₃), 0.97 (t, 18H; Si(CH₂CH₃)₃), 5.15 (brs, 2H; NH), 6.68 (dd, $^3J_{\text{Ha,Hb}} = 7.0$ Hz, $^4J_{\text{Ha,Hc}} = 1.4$ Hz, 2H; H^a, C₁₀H₆), 7.08–7.18 ppm (m, 4H; H^b + H^c, C₁₀H₆); ^{13}C NMR (50.32 MHz, CDCl₃, 295 K): $\delta = 4.5$ (Si(CH₂CH₃)₃), 7.1 (Si(CH₂CH₃)₃), 113.5 (CH; C₁₀H₆), 119.6 (CH; C₁₀H₆), 120.0 (C; C₁₀H₆), 125.7 (CH; C₁₀H₆), 137.3 (C; C₁₀H₆), 144.7 ppm (CN; C₁₀H₆); ^{29}Si NMR (39.76 MHz, CDCl₃, 295 K): $\delta = 8.1$ ppm; IR (CDCl₃): $\tilde{\nu} = 3370$ (br w), 3230 (vw), 3050 (w), 2960 (vs), 2910 (m), 2880 (s), 1575 (s), 1460 (m), 1415 (vs), 1310 (m), 1295 (s), 1260 (w), 1240 (w), 1100 (w), 1045 (s), 1010 (vs), 865 (m), 815 cm⁻¹ (s); elemental analysis calcd (%) for C₂₂H₃₈N₂Si₂ (386.73): C 68.33, H 9.90, N 7.24; found: C 68.22, H 10.21, N 7.00.

1,8-(iPr₃SiNH)₂C₁₀H₆ (1c): Yield: 10.8 g (91%); M.p.: 99°C ; ^1H NMR (400.13 MHz, CDCl₃, 295 K): $\delta = 1.15$ (d, $^3J_{\text{H,H}} = 7.6$ Hz, 36H; Si[CH(CH₃)₂]), 1.41 (sept, 6H; Si[CH(CH₃)₂]), 4.87 (brs, 2H; NH), 6.71 (dd, $^3J_{\text{Ha,Hb}} = 6.2$ Hz, $^4J_{\text{Ha,Hc}} = 2.3$ Hz, 2H; H^a, C₁₀H₆), 7.11–7.17 ppm (m, 4H; H^b + H^c, C₁₀H₆); ^{13}C NMR (100.61 MHz, CDCl₃, 295 K): $\delta = 13.0$

(Si[CH(CH₃)₂]), 18.7 (Si[CH(CH₃)₂]), 112.7 (CH; C₁₀H₆), 119.0 (C; C₁₀H₆), 119.1 (CH; C₁₀H₆), 125.5 (CH; C₁₀H₆), 137.3 (C; C₁₀H₆), 145.0 ppm (CN; C₁₀H₆); ^{29}Si NMR (39.76 MHz, CDCl₃, 295 K): $\delta = 6.5$ ppm; IR (KBr): $\tilde{\nu} = 3327$ (m), 3216 (br m), 3054 (m), 2941 (vs), 2864 (vs), 1902 (w), 1576 (s), 1511 (m), 1464 (vs), 1419 (s), 1289 (vs), 1045 (s), 1014 (s), 883 (s), 862 (m), 824 (m), 764 (m), 744 (m), 676 (m), 627 (m), 516 cm⁻¹ (m); elemental analysis calcd (%) for C₂₈H₅₀N₂Si₂ (470.89): C 71.42, H 10.70, N 5.95; found: C 71.30, H 10.60, N 5.86.

1,8-(Me₂tBuSiNH)₂C₁₀H₆ (1d): Yield: 11.0 g (86%); m.p. 72°C ; ^1H NMR (200.13 MHz, CDCl₃, 295 K): $\delta = 0.24$ (s, 12H; Si(CH₃)₂), 0.98 (s, 18H; SiC(CH₃)₃), 5.22 (brs, 2H; NH), 6.76 (dd, $^3J_{\text{Ha,Hb}} = 6.9$ Hz, $^4J_{\text{Ha,Hc}} = 2.1$ Hz, 2H; H^a, C₁₀H₆), 7.15–7.22 ppm (m, 4H; H^b + H^c, C₁₀H₆); ^{13}C NMR (50.32 MHz, CDCl₃, 295 K): $\delta = -3.7$ (Si(CH₃)₂), 18.9 (SiC(CH₃)₃), 27.0 (SiC(CH₃)₃), 115.2 (CH; C₁₀H₆), 119.9 (CH; C₁₀H₆), 120.8 (C; C₁₀H₆), 125.4 (CH; C₁₀H₆), 137.2 (C; C₁₀H₆), 144.6 ppm (CN; C₁₀H₆); ^{29}Si NMR (39.76 MHz, CDCl₃, 295 K): $\delta = 9.2$ ppm; IR (KBr): $\tilde{\nu} = 3330$ (m), 3240 (s), 3030 (s), 2940 (s), 2920 (s), 2870 (m), 2840 (s), 1605 (m), 1570 (s), 1510 (m), 1460 (vs), 1410 (s), 1385 (m), 1355 (m), 1300 (m), 1250 (vs), 1035 (s), 1020 (s), 1000 (m), 830 (br vs), 770 (vs), 750 (s), 680 (m), 655 cm⁻¹ (s); elemental analysis calcd (%) for C₂₂H₃₈N₂Si₂ (386.73): C 68.33, H 9.90, N 7.24; found: C 67.99, H 9.60, N 7.14.

1,8-(Me₂PhSiNH)₂C₁₀H₆ (1e): Yield: 4.06 g (95%); m.p. 92°C ; ^1H NMR (200.13 MHz, CDCl₃, 295 K): $\delta = 0.50$ (s, 12H; Si(CH₃)₂), 5.70 (brs, 2H; NH), 6.65 (d, $^3J_{\text{Ha,Hb}} = 7.7$ Hz, 2H; H^a, C₁₀H₆), 7.11 (t, 2H; H^b, C₁₀H₆), 7.25 (d, 2H; H^c, C₁₀H₆), 7.37–7.42 (m, 6H; Si(C₆H₅)), 7.62–7.67 ppm (m, 4H; Si(C₆H₅)); ^{13}C NMR (50.32 MHz, CDCl₃, 295 K): $\delta = -1.5$ (Si(CH₃)₂), 115.6 (CH; C₁₀H₆), 120.4 (CH; C₁₀H₆), 120.8 (C; C₁₀H₆), 125.6 (CH; C₁₀H₆), 128.0 (CH; Si(C₆H₅)), 129.5 (CH; Si(C₆H₅)), 133.6 (CH; Si(C₆H₅)), 137.2 (C; Si(C₆H₅)), 138.1 (C; C₁₀H₆), 143.6 ppm (CN; C₁₀H₆); ^{29}Si NMR (39.76 MHz, CDCl₃, 295 K): $\delta = -4.2$ ppm; IR (KBr): $\tilde{\nu} = 3320$ (m), 3270 (br m), 3040 (w), 2950 (w), 1570 (vs), 1505 (m), 1460 (m), 1410 (s), 1335 (w), 1290 (vs), 1250 (vs), 1115 (vs), 1040 (vs), 1025 (s), 875 (s), 840 (br vs), 790 (s), 780 (s), 760 (s), 730 (s), 700 (s), 650 cm⁻¹ (s); elemental analysis calcd (%) for C₂₆H₃₀N₂Si₂ (426.71): C 73.18, H 7.09, N 6.57; found: C 72.96, H 7.03, N 6.42.

1,8-(MePh₂SiNH)₂C₁₀H₆ (1f): Yield: 4.89 g (89%); m.p. 101°C ; ^1H NMR (200.13 MHz, CDCl₃, 295 K): $\delta = 0.59$ (s, 6H; Si(CH₃)₂), 5.70 (brs, 2H; NH), 6.67 (dd, $^3J_{\text{Ha,Hb}} = 7.7$ Hz, $^4J_{\text{Ha,Hc}} = 1.1$ Hz, 2H; H^a, C₁₀H₆), 7.03 (t, 2H; H^b, C₁₀H₆), 7.22 (dd, 2H; H^c, C₁₀H₆), 7.29–7.46 (m, 12H; Si(C₆H₅)₂), 7.55–7.59 ppm (m, 8H; Si(C₆H₅)₂); ^{13}C NMR (50.32 MHz, CDCl₃, 295 K): $\delta = -2.8$ (Si(CH₃)₂), 115.3 (CH; C₁₀H₆), 120.1 (C; C₁₀H₆), 120.2 (CH; C₁₀H₆), 125.6 (CH; C₁₀H₆), 128.0 (CH; Si(C₆H₅)₂), 129.8 (CH; Si(C₆H₅)₂), 134.6 (CH; Si(C₆H₅)₂), 135.7 (C; Si(C₆H₅)₂), 137.0 (C; C₁₀H₆), 143.2 ppm (CN; C₁₀H₆); ^{29}Si NMR (39.76 MHz, CDCl₃, 295 K): $\delta = -11.7$ ppm; IR (KBr): $\tilde{\nu} = 3320$ (m), 3230 (br w), 3060 (w), 3040 (w), 3000 (w), 2960 (vw), 1570 (vs), 1500 (m), 1460 (s), 1425 (vs), 1295 (vs), 1255 (s), 1110 (vs), 1045 (s), 1030 (m), 880 (m), 840 (m), 820 (m), 795 (s), 770 (m), 730 (s), 695 cm⁻¹ (vs); elemental analysis calcd (%) for C₃₆H₃₄N₂Si₂ (550.85): C 78.50, H 6.22, N 5.09; found: C 78.32, H 6.35, N 4.96.

General procedure for the preparation of the lithiated 1,8-bis(silylamino)naphthalenes: An equivalent amount of a solution of *n*-butyllithium in *n*-hexane (2.5M) was added dropwise at -30°C to a solution of the diamino naphthalene derivative in 100 mL of THF. After stirring for an hour at room temperature, the reaction mixture was briefly heated under reflux and subsequently, after concentration, stored at -35°C . The lithium amides were isolated as pale yellow, crystalline solids.

[1,8-(Me₃SiN)Li(thf)₂C₁₀H₆](THF) (2a): Yield: 40.9 g (92%); m.p. 82°C (decomp); ^1H NMR (200.13 MHz, C₆D₆, 295 K): $\delta = 0.45$ (s, 18H; Si(CH₃)₃), 1.08 (m, 12H; CH₂CH₂O), 3.28 (m, 12H; CH₂CH₂O), 6.77 (dd, $^3J_{\text{Ha,Hb}} = 7.2$ Hz, $^4J_{\text{Ha,Hc}} = 1.3$ Hz, 2H; H^a, C₁₀H₆), 7.13–7.32 ppm (m, 4H; H^b + H^c, C₁₀H₆); ^{13}C NMR (50.32 MHz, C₆D₆, 295 K): $\delta = 2.4$ (Si(CH₃)₃), 25.3 (CH₂CH₂O), 68.3 (CH₂CH₂O), 114.3 (CH; C₁₀H₆), 115.2 (CH; C₁₀H₆), 125.8 (C; C₁₀H₆), 126.6 (CH; C₁₀H₆), 140.8 (C; C₁₀H₆), 157.8 ppm (CN; C₁₀H₆); ^7Li NMR (77.77 MHz, C₆D₆, 295 K): $\delta = -0.60$ ppm; ^{29}Si NMR (39.76 MHz, C₆D₆, 295 K): $\delta = -13.0$; elemental analysis calcd (%) for C₂₈H₄₈Li₂N₂O₃Si₂ (530.75): C 63.36, H 9.12, N 5.28; found: C 63.08, H 9.01, N 5.02.

[1,8-(Et₃SiN)Li(thf)₂C₁₀H₆](THF) (2b): Yield: 4.32 g (87%); ^1H NMR (400.13 MHz, C₆D₆, 295 K): $\delta = 0.92$ (q, $^3J_{\text{H,H}} = 7.7$ Hz, 12H; Si(CH₂CH₃)₃), 1.10 (m, 12H; CH₂CH₂O), 1.19 (t, 18H; Si(CH₂CH₃)₃), 3.23 (m, 12H;

$\text{CH}_2\text{CH}_2\text{O}$), 6.78 (dd, $^3J_{\text{Ha,Hb}} = 7.4$ Hz, $^4J_{\text{Ha,Hc}} = 1.0$ Hz, 2H; H^a, C₁₀H₆), 7.11–7.25 ppm (m, 4H; H^b + H^c, C₁₀H₆); $^1\text{H}^{13}\text{C}$ NMR (100.61 MHz, C₆D₆, 295 K): $\delta = 7.3$ (Si(CH₂CH₃)₃), 8.9 (Si(CH₂CH₃)₃), 25.2 (CH₂CH₂O), 68.4 (CH₂CH₂O), 114.8 (CH; C₁₀H₆), 115.3 (CH; C₁₀H₆), 125.0 (C; C₁₀H₆), 126.5 (CH; C₁₀H₆), 140.7 (C; C₁₀H₆), 157.5 ppm (CN; C₁₀H₆); $^1\text{H}^7\text{Li}$ NMR (77.77 MHz, C₆D₆, 295 K): $\delta = -0.61$ ppm; $^1\text{H}^{29}\text{Si}$ NMR (39.76 MHz, C₆D₆, 295 K): $\delta = -4.7$ ppm; elemental analysis calcd (%) for C₃₄H₄₆Li₂N₂O₂Si₂ (614.92): C 66.41, H 9.84, N 4.56; found: C 64.73; H 9.67; N 4.65.

1,8-[(*i*Pr₃SiN)Li(thf)]₂C₁₀H₆ (2c): Yield: 5.71 g (91%); m.p. 56 °C (decomp). ^1H NMR (200.13 MHz, C₆D₆, 295 K): $\delta = 0.99$ (m, 8H; CH₂CH₂O), 1.30 (d, 36H; $^3J_{\text{H,H}} = 6.5$ Hz, Si(CH(CH₃)₂)₃), 1.44 (sept, 6H; Si(CH(CH₃)₂)₃), 2.99 (m, 8H; CH₂CH₂O), 6.88 (dd, $^3J_{\text{Ha,Hb}} = 7.3$ Hz, $^4J_{\text{Ha,Hc}} = 1.0$ Hz, 2H; H^a, C₁₀H₆), 7.17 (d, 2H; H^c, C₁₀H₆), 7.25 ppm (t, 2H; H^b, C₁₀H₆); $^1\text{H}^{13}\text{C}$ NMR (50.32 MHz, C₆D₆, 295 K): $\delta = 15.1$ (Si(CH(CH₃)₂)₃), 20.3 (Si(CH(CH₃)₂)₃), 25.1 (CH₂CH₂O), 68.5 (CH₂CH₂O), 115.6 (CH; C₁₀H₆), 116.5 (CH; C₁₀H₆), 124.8 (C; C₁₀H₆), 126.2 (CH; C₁₀H₆), 140.7 (C; C₁₀H₆), 157.7 ppm (CN; C₁₀H₆); $^1\text{H}^7\text{Li}$ NMR (77.77 MHz, C₆D₆, 295 K): $\delta = -0.80$ ppm; $^1\text{H}^{29}\text{Si}$ NMR (39.76 MHz, C₆D₆, 295 K): $\delta = -2.7$ ppm; elemental analysis calcd (%) for C₃₆H₆₄Li₂N₂O₂Si₂ (626.97): C 68.97, H 10.29, N 4.47; found: C 68.72, H 10.14, N 4.40.

1,8-[(Me₂tBuSiN)Li(thf)]₂C₁₀H₆ (2d): Yield: 9.83 g (100%); m.p. 67 °C (decomp); ^1H NMR (400.13 MHz, C₆D₆, 295 K): $\delta = 0.43$ (s, 12H; Si(CH₃)₂), 0.92 (m, 8H; CH₂CH₂O), 1.17 (s, 18H; SiC(CH₃)₃), 3.14 (m, 8H; CH₂CH₂O), 6.85 (dd, $^3J_{\text{Ha,Hb}} = 7.4$ Hz, $^4J_{\text{Ha,Hc}} = 1.4$ Hz, 2H; H^a, C₁₀H₆), 7.20 (dd, 2H; H^c, C₁₀H₆), 7.27 ppm (t, 2H; H^b, C₁₀H₆); $^1\text{H}^{13}\text{C}$ NMR (100.61 MHz, C₆D₆, 295 K): $\delta = -2.2$ (Si(CH₃)₂), 19.9 (SiC(CH₃)₃), 25.0 (SiC(CH₃)₃), 28.1 (CH₂CH₂O), 68.5 (CH₂CH₂O), 115.4 (CH; C₁₀H₆), 115.6 (CH; C₁₀H₆), 125.3 (C; C₁₀H₆), 126.4 (CH; C₁₀H₆), 140.7 (C; C₁₀H₆), 157.1 ppm (CN; C₁₀H₆); $^1\text{H}^7\text{Li}$ NMR (77.77 MHz, C₆D₆, 295 K): $\delta = -0.71$ ppm; $^1\text{H}^{29}\text{Si}$ NMR (39.76 MHz, C₆D₆, 295 K): $\delta = -4.5$ ppm; elemental analysis calcd (%) for C₃₀H₃₂Li₂N₂O₂Si₂ (542.81): C 66.38, H 9.66, N 5.16; found: C 66.27, H 9.67, N 5.05.

1,8-[(Me₂PhSiN)Li(thf)]₂C₁₀H₆ (2e): Yield: 1.12 g (96%); m.p. 84 °C (decomp); ^1H NMR (200.13 MHz, C₆D₆, 295 K): $\delta = 0.59$ (s, 12H; Si(CH₃)₂), 0.94 (m, 8H; CH₂CH₂O), 3.07 (m, 8H; CH₂CH₂O), 6.93 (dd, $^3J_{\text{Ha,Hb}} = 5.7$ Hz, $^4J_{\text{Ha,Hc}} = 3.1$ Hz, 2H; H^a, C₁₀H₆), 7.20–7.31 (m, 10H; H^b + H^c, C₁₀H₆/Si(C₆H₅)), 7.72–7.77 ppm (m, 4H; Si(C₆H₅)); $^1\text{H}^{13}\text{C}$ NMR (50.32 MHz, C₆D₆, 295 K): $\delta = 1.0$ (Si(CH₃)₂), 25.0 (CH₂CH₂O), 68.4 (CH₂CH₂O), 115.6 (CH; C₁₀H₆), 116.1 (CH; C₁₀H₆), 125.2 (C; C₁₀H₆), 126.6 (CH; C₁₀H₆), 128.3 (CH; Si(C₆H₅)), 128.6 (CH; Si(C₆H₅)), 133.6 (CH; Si(C₆H₅)), 140.6 (C; C₁₀H₆), 144.7 (C; Si(C₆H₅)), 156.5 ppm (CN; C₁₀H₆); $^1\text{H}^7\text{Li}$ NMR (77.77 MHz, C₆D₆, 295 K): $\delta = -0.56$ ppm; $^1\text{H}^{29}\text{Si}$ NMR (39.76 MHz, C₆D₆, 295 K): $\delta = -17.3$ ppm; elemental analysis calcd (%) for C₃₄H₄₄Li₂N₂O₂Si₂ (582.79): C 70.07, H 7.61, N 4.81; found: C 69.90, H 7.45, N 4.90.

1,8-[(MePh₂SiN)Li(thf)]₂C₁₀H₆ (2f): Yield: 2.98 g (77%); m.p. 84 °C (decomp); ^1H NMR (200.13 MHz, C₆D₆, 295 K): $\delta = 0.72$ (s, 6H; Si(CH₃)), 0.91 (m, 8H; CH₂CH₂O), 2.94 (m, 8H; CH₂CH₂O), 7.04–7.24 (m, 18H; C₁₀H₆/Si(C₆H₅)₂), 7.72–7.78 ppm (m, 8H; Si(C₆H₅)₂); $^1\text{H}^{13}\text{C}$ NMR (50.32 MHz, C₆D₆, 295 K): $\delta = -0.1$ (Si(CH₃)), 25.0 (CH₂CH₂O), 68.4 (CH₂CH₂O), 116.7 (CH; C₁₀H₆), 117.1 (CH; C₁₀H₆), 125.2 (C; C₁₀H₆), 126.4 (CH; C₁₀H₆), 128.1 (CH; Si(C₆H₅)₂), 128.7 (CH; Si(C₆H₅)₂), 134.8 (CH; Si(C₆H₅)₂), 140.3 (C; C₁₀H₆), 142.5 (C; Si(C₆H₅)₂), 156.0 ppm (CN; C₁₀H₆); $^1\text{H}^7\text{Li}$ NMR (77.77 MHz, C₆D₆, 295 K): $\delta = -0.35$ ppm; $^1\text{H}^{29}\text{Si}$ NMR (39.76 MHz, C₆D₆, 295 K): $\delta = -21.6$ ppm; elemental analysis calcd (%) for C₄₄H₄₈Li₂N₂O₂Si₂ (706.93): C 74.76, H 6.84, N 3.96; found: C 74.51, H 6.71, N 3.90.

Synthesis of 1,8-[Me₃SiN(Tl)]₂C₁₀H₆ (3a): Methylcyclohexane (40 mL), precooled at –30 °C, was added to a solid mixture of **2a** (1.00 g, 3.18 mmol) and TiCl₄ (1.52 g, 6.36 mmol). After the mixture had been stirred under strict exclusion of light for 18 h at room temperature, the solid LiCl formed in the reaction, together with other insoluble components, were separated by centrifugation, and the deep orange centrifugate was concentrated to about 10 mL and subsequently stored at –35 °C. Over the course of several days, the highly air- and moisture-sensitive, yellow-orange thallium amide **3a** precipitated as a microcrystalline solid. Yield: 1.53 g (68%); ^1H NMR (400.13 MHz, C₆D₆, 295 K): $\delta = 0.28$ (s, 18H; Si(CH₃)₃), 6.74 (dd, $^3J_{\text{Ha,Hb}} = 6.4$ Hz, $^4J_{\text{Ha,Hc}} = 2.8$ Hz, 2H; H^a, C₁₀H₆), 7.33–7.38 ppm (m, 4H; H^b + H^c, C₁₀H₆); $^1\text{H}^{13}\text{C}$ NMR (100.61 MHz, C₆D₆, 295 K): $\delta = 0.6$ (br, Si(CH₃)₃), 116.1 (br, CH, C₁₀H₆), 119.4 (CH; C₁₀H₆), 122.2 (br, C, C₁₀H₆), 126.9 (CH;

C₁₀H₆), 140.1 (C; C₁₀H₆), 151.0 ppm (br, CN, C₁₀H₆); $^1\text{H}^{29}\text{Si}$ NMR (39.76 MHz, C₆D₆O, 295 K): $\delta = -7.9$ ppm (br); elemental analysis calcd (%) for C₁₆H₂₄N₂Si₂Tl₂ (709.32): C 27.09, H 3.41, N 3.95, Tl 57.63; found: C 26.98, H 3.23, N 3.85, Tl 57.67.

General procedure for the preparation of the 4,9-bis(silylamino)perylenequinone-3,10-bis(silylimines): 1,4-Dioxane (75 mL), cooled at –60 °C, was added to a solid mixture of one of the lithiated 1,8-bis(silylamino)naphthalenes **2a–2f** (20.0 mmol) and TiCl₄ (9.59 g, 40.0 mmol). After warming to room temperature, the reaction mixture was stirred for 16–44 h at 90 °C (**2a**: 17 h; **2b**: 17.5 h; **2c**: 16 h; **2d**: 18 h; **2e**: 44 h; **2f**: 42 h). After removal of the solvent in vacuo, the residue was extracted with toluene (85 mL), the extract was concentrated to about 45 mL, and the dark green solution was stored at –35 °C. The 4,9-bis(silylamino)perylenequinone-3,10-bis(silylimines) (**4a–4f**) were obtained as black-green, microcrystalline solids.

[4,9-(Me₃SiNH)₂-3,10-(Me₃SiN)₂]C₂₀H₈ (4a): Yield: 2.99 g (76%); m.p. 212 °C (decomp); ^1H NMR (200.13 MHz, C₆D₆, 295 K): $\delta = 0.48$ (s, 36H; Si(CH₃)₃), 7.19 (d, $^3J_{\text{Ha,Hb}} = 9.7$ Hz, 4H; H^a, C₂₀H₈), 8.13 (d, 4H; H^b, C₂₀H₈), 14.13 ppm (s, 2H; NH); $^1\text{H}^{13}\text{C}$ NMR (50.32 MHz, C₆D₆, 295 K): $\delta = 1.4$ (Si(CH₃)₃), 112.2 (C; C₂₀H₈), 124.3 (C; C₂₀H₈), 125.4 (CH; C₂₀H₈), 126.4 (C; C₂₀H₈), 128.0 (CH; C₂₀H₈), 161.9 ppm (CN; C₂₀H₈); $^1\text{H}^{29}\text{Si}$ NMR (39.76 MHz, C₆D₆, 295 K): $\delta = -0.9$ ppm; IR (KBr): $\tilde{\nu} = 3455$ (vbr w), 3068 (w), 2955 (s), 2896 (m), 1622 (vs), 1590 (s), 1535 (vs), 1429 (m), 1356 (m), 1289 (m), 1249 (s), 1194 (s), 1071 (m), 963 (m), 836 (br vs), 778 (s), 759 (s), 686 (m), 663 (s), 630 (m), 480 cm⁻¹ (w); UV/Vis (*n*-pentane, $c = 10^{-5}$ mol L⁻¹): λ_{max} (lg ϵ) = 295.7 (5.09), 352.4 (4.05), 444.3 (4.82), 546.2 (3.88), 587.9 (4.31), 634.7 nm (4.53); elemental analysis calcd (%) for C₃₂H₄₆N₄Si₄ (599.09): C 64.16, H 7.74, N 9.35; found: C 63.81, H 7.53, N 9.28.

[4,9-(Et₃SiNH)₂-3,10-(Et₃SiN)₂]C₂₀H₈ (4b): Yield: 552 mg (78%); m.p. 224 °C (decomp); ^1H NMR (400.13 MHz, CDCl₃, 295 K): $\delta = 0.90$ (q, $^3J_{\text{H,H}} = 7.6$ Hz, 24H; Si(CH₂CH₃)₃), 1.04 (t, 36H; Si(CH₂CH₃)₃), 7.14 (d, $^3J_{\text{Ha,Hb}} = 9.6$ Hz, 4H; H^a, C₂₀H₈), 8.37 (d, 4H; H^b, C₂₀H₈), 13.32 ppm (s, 2H; NH); $^1\text{H}^{13}\text{C}$ NMR (100.61 MHz, CDCl₃, 295 K): $\delta = 5.7$ (Si(CH₂CH₃)₃), 7.4 (Si(CH₂CH₃)₃), 111.6 (C; C₂₀H₈), 123.7 (C; C₂₀H₈), 125.5 (CH; C₂₀H₈), 125.8 (C; C₂₀H₈), 127.1 (CH; C₂₀H₈), 161.8 ppm (CN; C₂₀H₈); $^1\text{H}^{29}\text{Si}$ NMR (39.76 MHz, CDCl₃, 295 K): $\delta = 4.8$ ppm; IR (KBr): $\tilde{\nu} = 3424$ (br s), 3054 (w), 2954 (vs), 2917 (s), 2873 (s), 1623 (s), 1587 (m), 1532 (s), 1461 (s), 1418 (m), 1291 (m), 1250 (m), 1195 (m), 1045 (m), 1014 (m), 975 (m), 802 (m), 777 (m), 742 (m), 588 (w), 457 cm⁻¹ (w); elemental analysis calcd (%) for C₄₄H₇₀N₄Si₄ (767.41): C 68.87, H 9.19, N 7.30; found: C 68.39, H 9.02, N 7.11.

[4,9-(*i*Pr₃SiNH)₂-3,10-(*i*Pr₃SiN)₂]C₂₀H₈ (4c): Yield: 1.27 g (82%); m.p. 329 °C; ^1H NMR (200.13 MHz, CDCl₃, 295 K): $\delta = 1.18$ (d, $^3J_{\text{H,H}} = 7.3$ Hz, 72H; Si(CH(CH₃)₂)₃), 1.46 (sept, 12H; Si(CH(CH₃)₂)₃), 7.12 (d, $^3J_{\text{Ha,Hb}} = 9.9$ Hz, 4H; H^a, C₂₀H₈), 8.35 (d, 4H; H^b, C₂₀H₈), 12.62 ppm (s, 2H; NH); $^1\text{H}^{13}\text{C}$ NMR (50.32 MHz, CDCl₃, 295 K): $\delta = 14.2$ (Si(CH(CH₃)₂)₃), 18.9 (Si(CH(CH₃)₂)₃), 112.1 (C; C₂₀H₈), 123.7 (C; C₂₀H₈), 125.8 (C; C₂₀H₈), 126.5 (CH; C₂₀H₈), 126.6 (CH; C₂₀H₈), 162.3 ppm (CN; C₂₀H₈); $^1\text{H}^{29}\text{Si}$ NMR (39.76 MHz, CDCl₃, 295 K): $\delta = 4.0$ ppm; IR (KBr): $\tilde{\nu} = 3448$ (vbr w), 3078 (w), 2944 (br vs), 2889 (s), 2865 (vs), 1623 (vs), 1594 (m), 1533 (vs), 1464 (s), 1426 (m), 1381 (m), 1352 (m), 1291 (m), 1249 (s), 1193 (s), 1067 (m), 1015 (m), 994 (m), 883 (s), 823 (m), 788 (s), 764 (vs), 689 (s), 663 (s), 640 (s), 505 (m), 463 cm⁻¹ (m); UV/Vis (*n*-pentane, $c = 10^{-5}$ mol L⁻¹): λ_{max} (lg ϵ) = 298.3 (5.09), 355.8 (4.16), 376.7 (4.28), 449.2 (4.90), 547.5 (3.95), 589.2 (4.35), 637.5 nm (4.56); elemental analysis calcd (%) for C₃₆H₉₄N₄Si₄ (935.73): C 71.88, H 10.13, N 5.99; found: C 71.39, H 10.09, N 5.91.

[4,9-(Me₂tBuSiNH)₂-3,10-(Me₂tBuSiN)₂]C₂₀H₈ (4d): Yield: 3.65 g (79%); m.p. 252 °C (decomp); ^1H NMR (200.13 MHz, CDCl₃, 295 K): $\delta = 0.41$ (s, 24H; Si(CH₃)₂), 1.00 (s, 36H; SiC(CH₃)₃), 7.21 (d, $^3J_{\text{Ha,Hb}} = 9.8$ Hz, 4H; H^a, C₂₀H₈), 8.38 (d, 4H; H^b, C₂₀H₈), 13.42 ppm (s, 2H; NH); $^1\text{H}^{13}\text{C}$ NMR (50.32 MHz, CDCl₃, 295 K): $\delta = -2.1$ (Si(CH₃)₂), 19.2 (SiC(CH₃)₃), 26.9 (SiC(CH₃)₃), 111.6 (C; C₂₀H₈), 123.7 (C; C₂₀H₈), 125.7 (C; C₂₀H₈), 126.0 (CH; C₂₀H₈), 127.1 (CH; C₂₀H₈), 161.8 ppm (CN; C₂₀H₈); $^1\text{H}^{29}\text{Si}$ NMR (39.76 MHz, C₆D₆, 295 K): $\delta = 4.9$ ppm; IR (KBr): $\tilde{\nu} = 3420$ (br vw), 3060 (vw), 2940 (m), 2920 (m), 2840 (m), 1615 (s), 1530 (s), 1350 (m), 1240 (m), 1190 (m), 1065 (m), 1000 (w), 825 (br vs), 800 (s), 770 (m), 680 cm⁻¹ (w); UV/Vis (*n*-pentane, $c = 10^{-5}$ mol L⁻¹): λ_{max} (lg ϵ) = 295.8 (5.10), 352.5 (4.06), 443.3 (4.83), 545.8 (3.89), 587.5 (4.31), 635.0 nm (4.53); elemental analysis calcd (%) for C₄₄H₇₀N₄Si₄ (767.41): C 68.87, H 9.19, N 7.30; found: C 68.66, H 9.40, N 6.99.

[4,9-(Me₂PhSiNH)₂-3,10-(Me₂PhSiN)₂]C₂₀H₈ (4e): Yield: 372 mg (77%); m.p. 209 °C (decomp); ^1H NMR (400.13 MHz, CDCl₃, 295 K): $\delta = 0.58$ (s,

24H; Si(CH₃)₂, 7.04 (d, ³J_{Ha,Hb} = 9.8 Hz, 4H; H^a, C₂₀H₈), 7.32–7.37 (m, 12H; Si(C₆H₅)₂), 7.60–7.68 (m, 8H; Si(C₆H₅)₂), 8.23 (d, 4H; H^b, C₂₀H₈), 14.02 ppm (s, 2H; NH); [¹H]¹³C NMR (100.61 MHz, CDCl₃, 295 K): δ = 0.1 (Si(CH₃)₂), 111.6 (C; C₂₀H₈), 123.9 (C; C₂₀H₈), 125.7 (CH; C₂₀H₈), 127.6 (CH; C₂₀H₈), 128.0 (CH; Si(C₆H₅)₂), 129.0 (C; C₂₀H₈), 129.3 (CH; Si(C₆H₅)₂), 133.7 (CH; Si(C₆H₅)₂), 139.1 (C; Si(C₆H₅)₂), 161.9 ppm (CN; C₂₀H₈); [¹H]²⁹Si NMR (39.76 MHz, CDCl₃, 295 K): δ = -8.1 ppm; IR (KBr): $\tilde{\nu}$ = 3386 (vbr s), 3066 (m), 3051 (m), 2955 (m), 2897 (w), 1954 (w), 1622 (vs), 1590 (s), 1522 (vs), 1426 (s), 1356 (m), 1294 (m), 1251 (s), 1202 (s), 1113 (s), 1070 (m), 831 (vs), 699 (s), 669 (m), 486 (m), 469 cm⁻¹ (m); elemental analysis calcd (%) for C₅₂H₅₄N₄Si₄ (847.37): C 73.71, H 6.42, N 6.61; found: C 73.30, H 6.29, N 6.48.

[4,9-(MePh₂SiNH)₂-3,10-(MePh₂SiN)]₂C₂₀H₈ (4f): Yield: 1.13 g (75 %); m.p. 203 °C (decomp); ¹H NMR (200.13 MHz, CDCl₃, 295 K): δ = 0.57 (s, 12H; Si(CH₃)₂), 7.02 (d, ³J_{Ha,Hb} = 9.8 Hz, 4H; H^a, C₂₀H₈), 7.26–7.38 (m, 24H; Si(C₆H₅)₂), 7.59–7.63 (m, 16H; Si(C₆H₅)₂), 8.13 (d, 4H; H^b, C₂₀H₈), 14.19 ppm (s, 2H; NH); [¹H]¹³C NMR (50.32 MHz, CDCl₃, 295 K): δ = -1.0 (Si(CH₃)₂), 112.0 (C; C₂₀H₈), 124.0 (C; C₂₀H₈), 126.1 (CH; C₂₀H₈), 127.7 (CH; C₂₀H₈), 127.9 (CH; Si(C₆H₅)₂), 129.0 (C; C₂₀H₈), 129.5 (CH; Si(C₆H₅)₂), 134.7 (CH; Si(C₆H₅)₂), 136.9 (C; Si(C₆H₅)₂), 162.2 ppm (CN; C₂₀H₈); [¹H]²⁹Si NMR (39.76 MHz, CDCl₃, 295 K): δ = -15.2 ppm; IR (KBr): $\tilde{\nu}$ = 3382 (vbr m), 3066 (m), 3046 (m), 3020 (m), 2955 (m), 1958 (w), 1888 (w), 1824 (w), 1774 (w), 1620 (vs), 1523 (vs), 1427 (s), 1354 (m), 1290 (m), 1251 (s), 1199 (m), 1111 (s), 1070 (m), 821 (s), 792 (vs), 725 (s), 699 (s), 642 (m), 484 (m), 449 cm⁻¹ (m); UV/Vis (*n*-pentane, *c* = 10⁻⁵ mol L⁻¹): λ_{max} (lg ε) = 266.7 (4.65), 296.7 (5.05), 315.0 (4.75), 330.0 (4.66), 347.5 (4.65), 451.7 (4.79), 540.8 (4.00), 582.5 (4.26), 630.8 nm (4.40); elemental analysis calcd (%) for C₇₂H₆₂N₄Si₄ (1095.65): C 78.93, H 5.70, N 5.11; found: C 78.47, H 5.96, N 4.90.

In situ synthesis of 1,8-[(NpN)Li(thf)]₂C₁₀H₆ and its conversion to [4,9-(NpNH)₂-3,10-(NpN)]₂C₂₀H₈ (6a) (Np = neopentyl): A solution of butyllithium in hexanes (2.5 M, 1.00 mL, 2.50 mmol) was slowly added to a cooled (-70 °C) solution of 1,8-bis(neopentylamino)naphthalene (**5a**, 347 mg, 1.20 mmol) in THF (20 mL). After the reaction mixture had been stirred at ambient temperature for 24 h and briefly heated to reflux, the solvents were removed in vacuo. The yellow, oily residue contained the bis-thf adduct of the lithium amide 1,8-[(NpN)Li(thf)]₂C₁₀H₆ in high purity, and was used as such in the subsequent reaction step. Yield of the crude product: 538 mg (99 %); ¹H NMR (200.13 MHz, C₆D₆, 295 K): δ = 1.17 (s, 18H; C(CH₃)₃), 1.17 (m, 8H; CH₂CH₂O), 3.01 (s, 4H; CH₂), 3.34 (m, 8H; CH₂CH₂O), 6.47 (d, ³J_{Ha,Hb} = 7.8 Hz, 2H; H^a, C₁₀H₆), 7.12 (d, 2H; H^c, C₁₀H₆), 7.46 ppm (t, 2H; H^b, C₁₀H₆).

1,4-Dioxane (40 mL), precooled at -60 °C, was added to a mixture of the lithium amide 1,8-[(NpN)Li(thf)]₂C₁₀H₆ (538 mg, 1.18 mmol) and solid TiCl₄ (576 mg, 2.40 mmol). After warming to room temperature, the reaction mixture was stirred at 95 °C for 20 h. Upon removal of the solvent in vacuo, the residue was extracted with toluene (40 mL) and the solvent in the extract was evaporated again under vacuum. The product mixture was then separated by column chromatography (silica 60, CH₂Cl₂/*n*-hexane: 1:3) and the perylene derivative **6a** was isolated as a black-green solid with a purple lustre. The compound's solubility in organic solvents was significantly lower than those of the silylated perylenes. Yield: 49 mg (21 %); ¹H NMR (200.13 MHz, C₆D₆, 295 K): δ = 1.14 (s, 36H; C(CH₃)₃), 3.45 (s, 8H; CH₂), 7.33 (d, ³J_{Ha,Hb} = 10.0 Hz, ⁴J_{Ha,Hc} = 1.5 Hz, 4H; H^a, C₂₀H₈), 8.33 (d, 4H; H^b, C₂₀H₈), 13.57 ppm (s, 2H; NH), IR (C₆D₆): $\tilde{\nu}$ = 3496 (br w), 2957 (br vs), 2928 (br vs), 2865 (s), 1627 (s), 1606 (s), 1525 (s), 1476 (m), 1390 (m), 1261 (s), 1196 (m), 1097 (br m), 1015 (br m), 791 cm⁻¹ (m); elemental analysis calcd (%) for C₄₀H₅₄N₄ (590.90): C 81.31, H 9.21, N 9.48; found: C 81.59, H 9.42, N 9.11.

Preparation of 3,4,9,10-(Me₂SiNH)₂C₂₀H₈ (7a) and 3,4,9,10-(Me₂tBu-SiNH)₂C₂₀H₈ (7d): A solution of **4a** or **4d** (0.50 mmol) in THF (35 mL) was slowly added to Na/Hg (Na: 1.00 mmol) at ambient temperature. After stirring for 24 h at room temperature, the deep blue solution that had formed during this period was decanted from the metallic mercury. After the mixture had been cooled to -55 °C, a solution of Et₃NHCl (138 mg, 1.00 mmol) in THF (15 mL) was added. After the mixture had then been stirred for another 18 h at ambient temperature, the solvent was removed in vacuo. The solid residue was extracted with toluene (75 mL), and the red, highly fluorescent solution was concentrated to 5 mL. Compounds **7a** and **7d** were obtained as highly air-sensitive, red, microcrystalline solids after

storage at -35 °C for several days. Yields: **7a**: 123 mg (41 %); **7d**: 192 mg (50 %).

Compound 7a: ¹H NMR (200.13 MHz, C₆D₆, 295 K): δ = 0.22 (s, 36H; Si(CH₃)₂), 5.43 (brs, 4H; NH), 6.72 (d, ³J_{Ha,Hb} = 8.1 Hz, 4H; H^a, C₂₀H₈), 7.88 ppm (d, 4H; H^b, C₂₀H₈); elemental analysis calcd (%) for C₃₂H₄₈N₄Si₄ (601.10): C 63.94, H 8.05, N 9.32; found: C 63.61, H 8.27, N 9.11.

Compound 7d: ¹H NMR (200.13 MHz, C₆D₆, 295 K): δ = 0.22 (s, 24H; Si(CH₃)₂), 0.97 (s, 36H; SiC(CH₃)₃), 5.29 (brs, 4H; NH), 6.83 (d, ³J_{Ha,Hb} = 7.9 Hz, 4H; H^a, C₂₀H₈), 7.83 ppm (d, 4H; H^b, C₂₀H₈); elemental analysis calcd (%) for C₄₄H₇₂N₄Si₄ (769.42): C 68.69, H 9.43, N 7.28; found: C 68.44, H 9.17, N 7.03.

Stoichiometric reaction between 3a and 7a: Solid **3a** (21 mg, 0.03 mmol) and solid **7a** (18 mg, 0.03 mmol) were placed in an NMR tube, and C₆D₆ (0.5 mL) was added. An immediate change of color from orange to dark green was observed, with the concomitant precipitation of thallium powder. After centrifugation of the precipitate to the top of the sealed NMR tube a ¹H NMR spectrum was recorded, indicating the presence of **1a** and **4a** as the only reaction products.

Synthesis of [4,9-(NH₂)₂-3,10-(NH)₂]C₂₀H₈ (8): KF (1.45 g, 25.0 mmol) dissolved in water (10 mL) was added at room temperature to a solution of compound **4a** (3.57 g, 5.96 mmol) in methanol (110 mL). A catalytic amount of [2,2,2]-cryptand was added to the reaction mixture, which was stirred for 26 h. The solid which precipitated was isolated by filtration on a G3-frit and then washed with methanol (80 mL), water (50 mL), acetone (40 mL) and, finally, *n*-pentane (40 mL). Drying of the solid under high vacuum in an ultrasonic bath at 40 °C for several hours gave the pure product [4,9-(NH₂)₂-3,10-(NH)₂]C₂₀H₈ (**8**). Yield: 1.83 g (99 %); m.p. 356 °C (decomp); ¹H NMR (400.13 MHz, (CD₃)₂SO, 295 K): δ = 7.16 (d, ³J_{Ha,Hb} = 9.8 Hz, 4H; H^a, C₂₀H₈), 8.47 (d, 4H; H^b, C₂₀H₈), 8.65 ppm (brs, 6H; NH/NH₂); [¹H]¹³C NMR (100.61 MHz, (CD₃)₂SO, 295 K): δ = 105.7 (C; C₂₀H₈), 123.0 (C; C₂₀H₈), 125.0 (C; C₂₀H₈), 125.4 (CH; C₂₀H₈), 127.3 (CH; C₂₀H₈), 159.6 ppm (CN; C₂₀H₈); IR (KBr): $\tilde{\nu}$ = 3444 (vbr m), 3384 (vbr m), 3252 (m), 3232 (m), 3057 (vs), 1626 (vs), 1608 (s), 1517 (vs), 1408 (m), 1288 (m), 1260 (w), 1198 (vs), 1039 (m), 921 (m), 843 (m), 818 (s), 628 (m), 497 cm⁻¹ (m); UV/Vis (DMSO, *c* = 10⁻⁵ mol L⁻¹): λ_{max} (lg ε) = 289.0 (4.72), 425.9 (4.45), 454.3 (4.19), 524.5 (3.50), 562.9 (3.84), 608.0 nm (3.97); emission (λ_{ex} = 426 nm, DMSO, *c* = 10⁻⁵ mol L⁻¹): λ_{max} = 635, 686; MS: *m/z* (I): 310.3 (100) [M]⁺, 283.2 (23) [M - CHN]⁺, 256.2 (22) [M - 2CHN]⁺, 155.1 (14) [½M]⁺, 128.1 (37) [½(M - 2CHN)]⁺; elemental analysis calcd (%) for C₂₀H₁₄N₄ (310.36): C 77.40, H 4.55, N 18.05; found: C 77.23, H 4.40, N 17.99.

Synthesis of [(bpy)₂Ru₂[μ₂-N,N'-N''-N'''-[4,9-(NH₂)₂-3,10-(NH)₂]C₂₀H₈]-PF₆]₂ (9): Acetone (50 mL) was added to a mixture of [Ru(bpy)₂Cl]₂(H₂O)₂ (500 mg, 0.96 mmol) and AgPF₆ (486 mg, 1.92 mmol). After stirring at room temperature under exclusion of light for 24 h the resulting deep orange suspension was slowly added, through a layer of flame-dried Celite on a G3 frit, to a mixture of **8** (142 mg, 0.46 mmol) in acetone (20 mL). The remaining residue from the frit was extracted twice with acetone (2 × 25 mL). The reaction mixture was then heated under reflux for 91 h, subsequently cooled to room temperature, and centrifuged. An aqueous solution of NH₄PF₆ (660 mg, 4.05 mmol) in H₂O (50 mL) was added to the blue-violet centrifugate. After concentration in vacuo, the reaction mixture was stirred at ambient temperature for 45 h and, after addition of 2-propanol (60 mL) and a small amount of zinc powder, for another 24 h. After concentration in vacuo, the solid precipitate was separated by filtration and washed first with degassed H₂O and then with diethyl ether. After drying (vacuum line), compound **9** was obtained as a microcrystalline, violet-blue solid. Yield: 466 mg (59 %); m.p. 292 °C (decomp). ¹H NMR (400.13 MHz, CD₃CN, 295 K): δ = 6.86 (br d, ³J_{Ha,Hb} = 10.0 Hz, 4H; C₂₀H₈/2H; C₁₀H₈N₂), 7.06 (d, *J*_{H,H} = 4.7 Hz, 2H; C₁₀H₈N₂), 7.14 (d, *J*_{H,H} = 5.0 Hz, 2H; C₁₀H₈N₂), 7.35 (d, *J*_{H,H} = 5.0 Hz, 2H; C₁₀H₈N₂), 7.50–7.56 (m, 4H; C₁₀H₈N₂), 7.66–7.72 (m, 4H; C₁₀H₈N₂), 7.87 (t, *J*_{H,H} = 7.9 Hz, 2H; C₁₀H₈N₂), 7.89 (t, *J*_{H,H} = 7.9 Hz, 2H; C₁₀H₈N₂), 8.12 (dd, *J*_{H,H} = 7.9 Hz, *J*_{H,H} = 3.8 Hz, 2H; C₁₀H₈N₂), 8.14 (dd, *J*_{H,H} = 7.9 Hz, *J*_{H,H} = 3.8 Hz, 2H; C₁₀H₈N₂), 8.37 (d, *J*_{H,H} = 7.6 Hz, 2H; C₁₀H₈N₂), 8.42 (d, *J*_{H,H} = 7.6 Hz, 2H; C₁₀H₈N₂), 8.56 (d, *J*_{H,H} = 7.6 Hz, 2H; C₁₀H₈N₂), 8.61 (d, *J*_{H,H} = 7.6 Hz, 2H; C₁₀H₈N₂), 9.13 ppm (d, ³J_{Ha,Hb} = 10.0 Hz, 4H; C₂₀H₈); [¹H]¹³C NMR (100.61 MHz, CD₃CN, 295 K): δ = 123.6 (CH; C₁₀H₈N₂), 123.7 (CH; C₁₀H₈N₂), 124.5 (CH; C₁₀H₈N₂), 124.6 (CH; C₁₀H₈N₂), 127.8 (CH; C₁₀H₈N₂), 128.5 (CH; C₁₀H₈N₂), 140.8 (CH; C₁₀H₈N₂), 142.0 (CH; C₁₀H₈N₂), 154.2 (C; C₂₀H₈), 154.7 (CH; C₂₀H₈), 155.5 (br, C, C₁₀H₈N₂), 155.6 (br, C, C₁₀H₈N₂), 156.2 (C; C₂₀H₈),

156.5 (C; C₂₀H₈), 158.4 (C; C₂₀H₈), 158.6 ppm (C; C₂₀H₈); ¹H³¹P NMR (161.98 MHz, (CD₃)₂CO, 295 K): δ = -144.1 ppm (sept, J_{PF} = 709 Hz, PF₆⁻); ¹H¹⁹F NMR (376.50 MHz, (CD₃)₂CO, 295 K): δ = -72.0 ppm (d, PF₆⁻); IR (KBr): $\tilde{\nu}$ = 3448 (vbr m), 3285 (m), 3089 (w), 2963 (w), 1631 (m), 1606 (m), 1467 (m), 1447 (m), 1396 (w), 1315 (w), 1263 (w), 1244 (w), 1187 (w), 1164 (w), 1035 (w), 841 (br vs), 763 (s), 733 (m), 663 (w), 558 cm⁻¹ (s); UV/Vis (CH₃CN, c = 10⁻⁵ mol L⁻¹, Ru(II)/Ru(III): λ_{max} (lg ε) = 216.1 (5.22), 286.0 (5.17), 359.3 (4.69), 585.9 nm (3.95); MS: m/z: 641.1 [M+1PF₆⁻]³⁺, 567.5 [M]²⁺, 427.1 [M+1PF₆⁻]⁴⁺, 378.5 [M]³⁺, 284.3 [M]⁴⁺; elemental analysis calcd (%) for C₆₀H₄₆F₂₄N₁₂P₄Ru₂ (1717.10): C 41.97, H 2.70, N 9.79, Ru 11.77; found: C 41.74, H 2.63, N 9.57, Ru 11.44.

Photophysical and electrochemical studies:

Emission spectra were recorded on a SPEX Fluorolog I (1681) instrument equipped with an R928 photomultiplier (Products for Research). Emission spectra were measured on dilute solutions with a 490 nm (emission-path) cut-off filter. No corrections were applied to the emission spectra. For determination of the emission quantum yields, by the "optical dilute method",^[38] [Ru(bpy)₃] in air-saturated acetonitrile (Φ_{em} = 0.016)^[39] was used as a standard. The excitation wavelength was 450 nm, and the optical density of both the reference and the sample was adjusted to 0.1 (1 cm) at this wavelength. Absorption spectra were recorded on a Hewlett Packard 8453 diode array spectrophotometer, with 1 nm bandwidth. Time-resolved emission and transient absorption spectra were obtained with a gated Optical Multi-channel Analyzer (OMA IV) from EG&G Instruments similar to that described earlier.^[40] As excitation and white probe sources, a tuneable Coherent Infinity laser (1 ns pulses FWHM) and an EG&G Xe flash lamp (X 504), respectively, were used. The excitation beam was at a right angle to the probing beam. The probing path length was 1 cm. Samples were adjusted to an absorption of 0.5 (1 cm) at the excitation wavelength (450 nm). The laser power was about 3 mJ per pulse (0.2 cm²).

The subnanosecond luminescence lifetimes were measured with time-correlated single-photon counting, by use of a Hamamatsu microchannel plate (R 3809) detector in a set-up slightly modified from that previously described,^[41] with a frequency-doubled DCM dye laser, synchronously pumped with a mode-locked Argon ion laser. This results in 324 nm 20 ps FWHM pulses. Decays were analysed with an in-house deconvolution program.

Spectroelectrochemistry was performed with an in-house optically transparent thin-layer electrochemical cell with quartz windows, similar to that described before.^[42] Cyclic voltammetry was performed with TBAPF₆ (0.1M) in freshly distilled dichloromethane as electrolyte, with ferrocene/ferricinium as internal standard. A concentration of 1 × 10⁻³ M was used. Spectroscopy grade solvents were used in all determinations, freshly distilled for electrochemistry.

X-ray crystallographic study of 2c, 4a and 4d

Data collection: X-ray intensity data were collected on a Siemens P4 diffractometer for **4a** and **4d**, and on a Stoe IPDS diffractometer for **2c**. Details of data collection, refinement and crystal data are listed in Table 1.

Table 1. X-Ray crystallographic and data processing parameters for complexes **2c**, **4a** and **4d**.

	2c	4a	4d
formula	C ₃₆ H ₆₄ Li ₂ N ₂ O ₂ Si ₂	C ₃₂ H ₄₆ N ₄ Si ₄	C ₄₄ H ₇₀ N ₄ Si ₄
M _r	626.95	599.09	767.40
crystal system	monoclinic	monoclinic	triclinic
space group	C2 (no. 5)	P2 ₁ /c (no. 14)	P1 (no. 2)
unit cell dimensions			
a [Å]	14.295(3)	13.727(17)	11.0336(15)
b [Å]	14.942(3)	10.587(10)	13.852(2)
c [Å]	19.098(4)	12.885(10)	15.485(2)
α [°]	-	-	84.411(8)
β [°]	111.88(3)	111.32(7)	79.200(10)
γ [°]	-	-	80.047(9)
U [Å ³]	3785.5(13)	1744(3)	2284.5(6)
Z	4	2	2
ρ _{calcd} [Mg m ⁻³]	1.100	1.141	1.116
radiation	MoK _α	MoK _α	MoK _α
wavelength [Å]	0.71073	0.71073	0.71073
μ [mm ⁻¹]	0.125	0.197	0.164
F(000)	1376	644	836
crystal size (mm)	0.50 × 0.25 × 0.25	0.72 × 0.44 × 0.32	0.60 × 0.50 × 0.32
θ-range [°]	2.30 to 24.00	1.59 to 18.00	1.34 to 25.00
limiting hkl indices	-16 ≤ h ≤ 16 -17 ≤ k ≤ 16 -21 ≤ l ≤ 21	-16 ≤ h ≤ 15 -12 ≤ k ≤ 1 -1 ≤ l ≤ 15	-13 ≤ h ≤ 13 -16 ≤ k ≤ 16 -18 ≤ l ≤ 18
reflections collected	13619	1652	16109
independent reflections (R _{int})	5790 (0.0567)	1198 (0.1955)	8055 (0.0591)
data/restraints/parameters	5790/64/411	925/60/181	7603/0/494
S on F ²	0.929	1.053	0.999
final R indices ^[a]			
[I > 2σ(I)]			
R ₁	0.0394	0.1063	0.0566
wR ₂	0.0902	0.2020	0.1252
(all data)			
R ₁	0.0595	0.2421	0.1110
wR ₂	0.0968	0.3195	0.1497
weights a, b ^[a]	0.0505, 0.0000	~0.1040, 0.0000	0.0700, 0.5765
max and min Δρ [e Å ⁻³]	0.343/~0.217	0.377/~0.257	0.663/~0.300

[a] S = [Σw(F_o² - F_c²)/(n - p)]², where n = number of reflections and p = total number of parameters, R₁ = Σ||F_o - |F_c||/Σ|F_o|, wR₂ = Σ[w(F_o² - F_c²)]/Σ[w(F_o²)]^{1/2}, w⁻¹ = [σ²(F_o)² + (aP)² + bP], P = [max(F_o², 0) + 2(F_c²)]/3.

Absorption corrections using psi-scans were applied to the data of **4d**, but not of **4a** or **2c**.

Structure solution and refinement:^[43-46] For compounds **2c**, **4a** and **4d**, the positions of the non-hydrogen atoms were located by direct methods and refinement was based on F². In two of the structures, **4d** and **2c**, the asymmetric unit consists of two independent half molecules, and in **4a** of one half molecule. In **4d** there are two independent centrosymmetric tetraaminoperylene molecules in the unit cells, and in **2c** there are two independent molecules of C₂ symmetry. Residual electron density close to Si(1) in **4d** was interpreted as due to a small (ca. 15%) disorder of this atom. Relatively high displacement parameters for the aliphatic carbon atoms in **4d**, and rather higher displacement parameters for the methyl groups in **4a** were consistent with some unresolved disorder of the tert-butyl and methyl substituents. Direct location of the two amino hydrogen atoms (one per half molecule) expected in the asymmetric unit of **4d** showed that they were disordered over the four nitrogen atoms, and they were therefore assigned half occupancy. Therefore, in **4a**, where these atoms could not be directly located, hydrogen atoms of half occupancy were assigned to calculated sites on each of the four nitrogen atoms of the asymmetric unit. Fixed isotropic displacement parameters of 0.10 Å² were assigned to the amino hydrogen atoms in **4a**, whilst in **4d** the values of these parameters for the four amino hydrogen atoms were tied to a common parameter which refined to 0.04 Å². The remaining hydrogen atoms for all three structures were placed in calculated positions with displacement parameters set equal to 1.2 U_{eq} (or 1.5 U_{eq} for methyl groups) of the parent carbon atoms. For the structures of **2c** and **4a**, chemically equivalent bond lengths in the two independent molecules were constrained to be equal

within an esd of 0.01 Å. In the final cycles of full-matrix, least-squares refinement, for all three structures, the non-hydrogen atoms were assigned anisotropic displacement parameters (except for Si(3) for the minor component of the disordered silicon atom in **4d**).

CCDC-180299 (**2c**), CCDC-180300 (**4a**), and CCDC-180301 (**4d**) contain the supplementary crystallographic data for this paper. These data can be obtained free of charge via www.ccdc.cam.ac.uk/conts/retrieving.html (or from the Cambridge Crystallographic Data Centre, 12 Union Road, Cambridge CB2 1EZ, UK; fax: (+44)1223-336033; or deposit@ccdc.cam.ac.uk).

Acknowledgements

We are grateful to the CNRS (France), the Institut Universitaire de France, the Deutsche Forschungsgemeinschaft and the EPSRC (UK), for funding. L.d.C. and R.M.W. thank Taasje Maharabiersing for his experimental contributions. L.H.G. thanks Ina Rüdener for experimental help and Dr. Markus Herderich for recording the electrospray mass spectrum of compound **9**, as well as one of the referees for helpful comments.

- [1] a) H. Zollinger, *Color Chemistry*, 2nd ed., VCH, Weinheim, **1991**;
b) W. Herbst, K. Hunger, *Industrial Organic Pigments, Production, Properties, Applications*, Wiley-VCH, Weinheim, **1997**.
- [2] a) H. Kaiser, J. Lindner, H. Langhals, *Chem. Ber.* **1991**, *124*, 529;
b) P. M. Kazmaier, R. Hoffmann, *J. Am. Chem. Soc.* **1994**, *116*, 9684;
c) R. Reisfeld, G. Seybold, *Chimia* **1990**, *44*, 295.
- [3] a) M. Sadrai, G. R. Bird, *Opt. Commun.* **1984**, *51*, 62; b) K. Kuriki, T. Kobayashi, N. Imai, T. Tamura, Y. Koike, Y. Okamoto, *Polym. Adv. Tech.* **2000**, *11*, 612.
- [4] a) D. R. Kearns, *Chem. Rev.* **1971**, *71*, 395; b) D. W. Cameron, A. G. Riches, *Aust. J. Chem.* **1997**, *50*, 409; c) H. G. Löhmannsröben, H. Langhals, *Appl. Phys. B* **1989**, *48*, 449.
- [5] a) R. L. Garwin, *Rev. Sci. Instr.* **1960**, *31*, 1010; b) A. Goetzberger, W. Greubel, *Appl. Phys.* **1977**, *14*, 123; c) C. W. Tang, *Appl. Phys. Lett.* **1986**, *48*, 183; d) M. Hiramoto, Y. Kishigami, M. Yokoyama, *Chem. Lett.* **1990**, 119; e) B. A. Gregg, *J. Phys. Chem.* **1996**, *100*, 852; f) D. A. Adams, J. Kerimo, D. B. O'Connor, P. F. Barbara, *J. Phys. Chem. A* **1999**, *103*, 10138; g) S. Ferrere, A. Zaban, B. A. Gregg, *J. Phys. Chem. B* **1997**, *101*, 4490; h) F. Würthner, *Nachr. Chem.* **2001**, *49*, 1284.
- [6] a) C. Göltner, D. Pressner, K. Müllen, H. W. Spiëß, *Angew. Chem.* **1993**, *105*, 1722; *Angew. Chem. Int. Ed. Engl.* **1993**, *32*, 1660; b) C. W. Struijk, A. B. Sieval, J. E. J. Dakhorst, M. van Dijk, P. Kimkes, R. B. M. Koehorst, H. Donker, T. J. Schaafsma, S. J. Picken, A. M. van de Craats, J. M. Warman, H. Zuilhof, E. J. R. Sudhölter, *J. Am. Chem. Soc.* **2000**, *122*, 11057; c) R. A. Cormier, B. A. Gregg, *J. Phys. Chem. B* **1997**, *101*, 11004; d) P. Schlichting, U. Rohr, K. Müllen, *J. Mater. Chem.* **1998**, *8*, 2561; e) B. A. Gregg, R. A. Cormier, *J. Phys. Chem. B* **1998**, *102*, 9952; f) R. A. Cormier, B. A. Gregg, *Chem. Mater.* **1998**, *10*, 1309; g) G. P. Wiederrecht, B. A. Yoon, M. R. Wasielewski, *Adv. Mater.* **2000**, *12*, 1533.
- [7] a) M. M. Labes, R. Sehr, M. Bose, *J. Chem. Phys.* **1960**, *33*, 868; b) H.-C. I. Kao, M. Jones, M. M. Labes, *J. Chem. Soc. Chem. Commun.* **1979**, 329; c) V. Gama, R. T. Henriques, G. Bonfait, M. Almeida, A. Meetsma, S. van Smaalen, J. L. de Boer, *J. Am. Chem. Soc.* **1992**, *114*, 1986.
- [8] a) H. Brockmann, E.-H. von Falkenhausen, A. Dorlars, *Naturwissenschaften* **1950**, *37*, 540; b) H. Brockmann, H. Eggers, *Angew. Chem.* **1955**, *22*, 706; c) H. Brockmann, *Proc. Chem. Soc.* **1957**, 304; d) A. Smirnov, D. B. Fulton, A. Andreotti, J. W. Petrich, *J. Am. Chem. Soc.* **1999**, *121*, 7979; e) T. G. Dax, H. Falk, *Monatsh. Chem.* **2000**, *131*, 1217; f) B. Immitzer, H. Falk, *Monatsh. Chem.* **2000**, *131*, 1167; g) T. G. Dax, C. Eitzlstorfer, H. Falk, *Monatsh. Chem.* **2000**, *131*, 1115.
- [9] a) M. Weng, M.-H. Zhang, T. Shen, *J. Chem. Soc. Perkin Trans. 2* **1997**, 2393; b) C. Wei-shin, C. Yuan-teng, W. Xiang-yi, E. Friedrichs, H. Puff, E. Breitmaier, *Liebigs Ann. Chem.* **1981**, 1880.
- [10] a) M. Wainwright, *Chem. Soc. Rev.* **1996**, 351; b) J. W. Lown, *Can. J. Chem.* **1997**, *75*, 99; c) M. J. Fehr, M. A. McCloskey, J. W. Petrich, *J. Am. Chem. Soc.* **1995**, *117*, 1833.
- [11] D. S. English, W. Zhang, G. A. Kraus, J. W. Petrich, *J. Am. Chem. Soc.* **1997**, *119*, 2980.
- [12] a) J. Lukáč, H. Langhals, *Chem. Ber.* **1983**, *116*, 3524; b) H. Langhals, *Chem. Ber.* **1985**, *118*, 4641; c) H. Langhals, *Chimia* **1994**, *48*, 503; d) L. Feiler, H. Langhals, K. Polborn, *Liebigs Ann. Chem.* **1995**, 1229; e) H. Langhals, J. Gold, *J. Prakt. Chem.* **1996**, 338, 654; f) H. Langhals, P. von Unold, M. Speckbacher, *Liebigs Ann. Chem., Recueil* **1997**, 467; g) H. Langhals, W. Jona, *Eur. J. Org. Chem.* **1998**, 847; h) H. Langhals, H. Jäschke, U. Ring, P. von Unold, *Angew. Chem.* **1999**, *111*, 143; *Angew. Chem. Int. Ed.* **1999**, *38*, 201; i) M. Adachi, Y. Nagao, *Chem. Mater.* **1999**, *11*, 2107; j) H. Langhals, F. Süßmeier, *J. Prakt. Chem.* **1999**, *341*, 309; k) H. Langhals, S. Kirner, *Eur. J. Org. Chem.* **2000**, 365; l) K. D. Belfield, K. J. Schafer, M. D. Alexander, Jr., *Chem. Mater.* **2000**, *12*, 1184; m) T. Sakamoto, C. Pac, *J. Org. Chem.* **2001**, *66*, 94; n) S. Demmig, H. Langhals, *Chem. Ber.* **1988**, *121*, 225; o) D. Dotcheva, M. Klapper, K. Müllen, *Macromol. Chem. Phys.* **1994**, *195*, 1905; p) H. Quante, P. Schlichting, U. Rohr, Y. Geerts, K. Müllen, *Macromol. Chem. Phys.* **1996**, *197*, 4029; q) U. Rohr, P. Schlichting, A. Böhm, M. Groß, K. Meerholz, C. Bräuchle, K. Müllen, *Angew. Chem.* **1998**, *110*, 1463; *Angew. Chem. Int. Ed.* **1998**, *37*, 1434.
- [13] a) F. O. Holtrup, G. R. J. Müller, H. Quante, S. De Feyter, F. C. De Schryver, K. Müllen, *Chem. Eur. J.* **1997**, *3*, 219; b) Y. Geerts, H. Quante, H. Platz, R. Mahrt, M. Hopmeier, A. Böhm, K. Müllen, *J. Mater. Chem.* **1998**, *8*, 2357; c) S. K. Lee, Y. Zu, A. Herrmann, Y. Geerts, K. Müllen, A. J. Bard, *J. Am. Chem. Soc.* **1999**, *121*, 3513; d) P. Schlichting, B. Duchscherer, G. Seisenberger, T. Basché, C. Bräuchle, K. Müllen, *Chem. Eur. J.* **1999**, *5*, 2388.
- [14] A. Zinke, E. Unterkreuter, *Monatsh. Chem.* **1919**, *40*, 405.
- [15] A. Zinke, W. Hirsch, E. Brozek, *Monatsh. Chem.* **1929**, *51*, 205.
- [16] K. W. Hellmann, C. H. Galka, I. Rüdener, L. H. Gade, I. J. Scowen, M. McPartlin, *Angew. Chem.* **1998**, *110*, 2053; *Angew. Chem. Int. Ed.* **1998**, *37*, 1948.
- [17] a) M. Tamano, S. Maki (Toyo Ink MFG Co., Ltd), EP 0965629A, **1999**;
b) S. Onikubo, M. Tamano (Toyo Ink MFG Co., Ltd), JP 2000150152A, **2000**;
c) S. Onikubo, M. Tamano (Toyo Ink MFG Co., Ltd), JP 2000150161A, **2000**;
d) M. Tamano, S. Onikubo (Toyo Ink MFG Co., Ltd), JP 2000068058A, **2000**.
- [18] K. W. Hellmann, C. H. Galka, L. H. Gade, A. Steiner, D. S. Wright, T. Kottke, D. Stalke, *Chem. Commun.* **1998**, 549.
- [19] π Interactions between Tl^I and aromatic rings have been observed in several cases; see for example: a) S. D. Waezsada, T. Belgardt, M. Noltemeyer, H. W. Roesky, *Angew. Chem.* **1994**, *106*, 1431; *Angew. Chem. Int. Ed. Engl.* **1994**, *33*, 1351; b) W. Frank, D. Kuhn, S. Müller-Becker, A. Ravazi, *Angew. Chem.* **1993**, *105*, 102; *Angew. Chem. Int. Ed. Engl.* **1993**, *32*, 90; c) M. D. Noiro, O. P. Anderson, S. H. Strauss, *Inorg. Chem.* **1987**, *26*, 2216; d) H. Schmidbauer, W. Bublak, B. Huber, J. Hofmann, G. Müller, *Chem. Ber.* **1989**, *122*, 102; e) C. H. Galka, L. H. Gade, *Inorg. Chem.* **1999**, *38*, 1038; f) C. H. Galka, D. J. M. Trösch, M. Schubart, L. H. Gade, I. J. Scowen, M. McPartlin, *Eur. J. Inorg. Chem.* **2000**, 2577.
- [20] C. H. Galka, D. J. M. Trösch, I. Rüdener, L. H. Gade, I. J. Scowen, M. McPartlin, *Inorg. Chem.* **2000**, *39*, 4615 and references therein.
- [21] R. E. Mulvey, *Chem. Soc. Rev.* **1998**, *27*, 339.
- [22] a) K. Gregory, P. von R Schleyer, R. Snaith, *Adv. Inorg. Chem.* **1991**, *37*, 47; b) R. E. Mulvey, *Chem. Soc. Rev.* **1991**, *20*, 167.
- [23] S. Daniele, C. Drost, B. Gerhus, S. M. Hawkins, P. B. Hitchcock, M. F. Lappert, P. G. Merle, S. G. Bott, *J. Chem. Soc., Dalton Trans.* **2001**, 3179.
- [24] a) H. Bock, C. Näther, Z. Havlas, *J. Am. Chem. Soc.* **1995**, *117*, 3869; b) C. Näther, H. Bock, Z. Havlas, T. Hauck, *Organometallics* **1998**, *17*, 4707.
- [25] R. B. Hammond, K. J. Roberts, E. D. L. Smith, R. Docherty, *J. Phys. Chem. B* **1999**, *103*, 7762.
- [26] a) F. Graser, E. Hädicke, *Liebigs Ann. Chem.* **1980**, 1994; b) F. Graser, E. Hädicke, *Liebigs Ann. Chem.* **1984**, 483; c) G. Klebe, F. Graser, E. Hädicke, J. Berndt, *Acta Crystallogr. Sect. B* **1989**, *45*, 69.
- [27] E. Hädicke, F. Graser, *Acta Crystallogr. Sect. C* **1986**, *42*, 189.
- [28] G. R. Desiraju, A. Gavezzotti, *J. Chem. Soc. Chem. Commun.* **1989**, 621.
- [29] K. W. Hellmann, L. H. Gade, A. Steiner, D. Stalke, F. Möller, *Angew. Chem.* **1997**, *109*, 99; *Angew. Chem. Int. Ed. Engl.* **1997**, *36*, 160.
- [30] W. E. Ford, P. V. Kamat, *J. Phys. Chem.* **1987**, *91*, 6373–6380.

- [31] H. Langhals, *Heterocycles* **1995**, *40*, 477–500.
- [32] S. L. Murov, I. Carmichael, G. L. Hug, *Handbook of Photochemistry*, Marcel Dekker Inc., New York **1993**.
- [33] a) A. Minsky, J. Klein, M. Rabinovitz, *J. Am. Chem. Soc.* **1981**, *103*, 4586; b) A. Minsky, A. Y. Meyer, M. Rabinovitz, *J. Am. Chem. Soc.* **1982**, *104*, 2475; c) M. Munakata, L. P. Wu, T. Kuroda-Sowa, M. Maekawa, Y. Suenaga, K. Sugimoto, *Inorg. Chem.* **1997**, *36*, 4903; d) L. P. Battaglia, C. Bellitto, M. R. Cramarossa, I. M. Vezzosi, *Inorg. Chem.* **1996**, *35*, 2390; e) L. Alcácer, H. Novais, F. Pedroso, S. Flandrois, C. Coulon, D. Chasseau, J. Gaultier, *Solid State Commun.* **1980**, *35*, 945; f) R. T. Henriques, L. Alcácer, J. P. Pouget, D. Jérôme, *J. Phys. C: Solid State Phys.* **1984**, *17*, 5197; g) R. T. Henriques, M. Almeida, M. J. Matos, L. Alcácer, C. Bourbonnais, *Synth. Met.* **1987**, *19*, 379; h) L. Alcácer, *Mol. Cryst. Liq. Cryst.* **1985**, *120*, 221; i) A. Domingos, R. T. Henriques, V. P. Gama, M. Almeida, A. Lopes Vieira, L. Alcácer, *Synth. Met.* **1989**, *27*, B411; j) V. Gama, M. Almeida, R. T. Henriques, I. C. Santos, A. Domingos, S. Ravy, J. P. Pouget, *J. Phys. Chem.* **1991**, *95*, 4263; k) V. Gama, R. T. Henriques, G. Bonfait, L. C. Pereira, J. C. Waerenborgh, I. C. Santos, M. T. Duarte, J. M. P. Cabral, M. Almeida, *Inorg. Chem.* **1992**, *31*, 2598; l) J. F. Bringley, B. A. Averill, *J. Chem. Soc. Chem. Commun.* **1987**, 399; m) H. Yamochi, G. Saito, T. Sugano, M. Kinoshita, C. Katayama, J. Tamaka, *Chem. Lett.* **1986**, 1303; n) M. Sadrai, G. R. Bird, J. A. Potenza, H. J. Schugar, *Acta Crystallogr. Sect. C* **1990**, *46*, 637; o) H. Imamura, S. Tsuchiya, *J. Catal.* **1981**, *72*, 383; p) H. Endres, H. J. Keller, B. Müller, D. Schweitzer, *Acta Crystallogr. Sect. C* **1985**, *41*, 607.
- [34] a) F. Würthner, A. Sautter, *Chem. Commun.* **2000**, 445; b) F. Würthner, A. Sautter, D. Schmid, P. J. A. Weber, *Chem. Eur. J.* **2001**, *7*, 894.
- [35] a) B. P. Sullivan, D. J. Salmon, T. J. Meyer, *Inorg. Chem.* **1978**, *17*, 3334; b) P. A. Lay, A. M. Sargeson, H. Taube, *Inorg. Synth.* **1986**, *24*, 291.
- [36] Reviews: a) M. D. Ward, *Chem. Soc. Rev.* **1995**, 121; b) D. E. Richardson, H. Taube, *Coord. Chem. Rev.* **1984**, *60*, 107; c) G. Blasse, *Struct. Bond.* **1991**, *76*, 153; d) T. J. Meyer, *Acc. Chem. Res.* **1978**, *11*, 94; selected references: e) D. E. Richardson, H. Taube, *Inorg. Chem.* **1981**, *20*, 1278; f) A. R. Rezvani, C. E. B. Evans, R. J. Crutchley, *Inorg. Chem.* **1995**, *34*, 4600; g) M. Beley, J.-P. Collin, J.-P. Sauvage, *Inorg. Chem.* **1993**, *32*, 4539; h) E. C. Constable, A. M. W. Cargill-Thompson, S. Greulich, *J. Chem. Soc. Chem. Commun.* **1993**, 1444; i) M. D. Ward, *Inorg. Chem.* **1996**, *35*, 1712; j) M. Haga, A. M. Bond, *Inorg. Chem.* **1991**, *30*, 475; k) V. Kasack, W. Kaim, H. Binder, J. Jordanov, E. Roth, *Inorg. Chem.* **1995**, *34*, 1924; l) A.-C. Ribou, J.-P. Launay, K. Takahashi, T. Nihira, S. Tarutani, C. W. Spangler, *Inorg. Chem.* **1994**, *33*, 1325; m) I. de S. Moreira, D. W. Franco, *Inorg. Chem.* **1994**, *33*, 1607; n) D. N. Marks, W. O. Siegl, *Inorg. Chem.* **1982**, *21*, 3140; o) R. W. Callahan, F. R. Keene, T. J. Meyer, D. J. Salmon, *J. Am. Chem. Soc.* **1977**, *99*, 1064; p) J. E. Sutton, H. Taube, *Inorg. Chem.* **1981**, *20*, 3125; q) S. Joss, H. Reust, A. Ludi, *J. Am. Chem. Soc.* **1981**, *103*, 981; r) A. J. Downard, G. E. Honey, L. F. Phillips, P. J. Steel, *Inorg. Chem.* **1991**, *30*, 2259; s) Y. Kim, C. M. Lieber, *Inorg. Chem.* **1989**, *28*, 3990; t) M. A. S. Aquino, F. L. Lee, E. J. Gabe, C. Bensimon, J. E. Greedan, R. J. Crutchley, *J. Am. Chem. Soc.* **1992**, *114*, 5130; u) K. A. Goldsby, T. J. Meyer, *Inorg. Chem.* **1984**, *23*, 3002.
- [37] M. B. Robin, P. Day, *Adv. Inorg. Chem. Radiochem.* **1967**, 247.
- [38] J. N. Demas, G. A. Crosby, *J. Phys. Chem.* **1971**, *75*, 991–1024.
- [39] J. V. Caspar, T. J. Meyer, *J. Am. Chem. Soc.* **1983**, *105*, 5583.
- [40] J. M. Haider, M. Chavarot, S. Weidner, I. Sadler, R. M. Williams, L. De Cola, Z. Pikramenou, *Inorg. Chem.* **2001**, *40*, 3912–3921.
- [41] D. Bebehaar, *Rev. Sci. Instrum.* **1986**, *57*, 116–125.
- [42] M. Krejčík, M. Danek, F. Hartl, *J. Electroanal. Chem.* **1991**, *317*, 179–187.
- [43] G. M. Sheldrick, *Acta Crystallogr. Sect. A* **1990**, *46*, 467.
- [44] G. M. Sheldrick, SHELXS-97, Program for Crystal Structure Solution, Universität Göttingen, **1997**.
- [45] G. M. Sheldrick, SHELXL-93, Program for Crystal Structure Refinement, Universität Göttingen, **1993**.
- [46] G. M. Sheldrick, SHELXL-97, Program for Crystal Structure Refinement, Universität Göttingen, **1997**.

Received: February 28, 2002 [F 3907]